Origin and hidden diversity within the poorly known Galápagos snake radiation (Serpentes: Dipsadidae)

Hussam Zaher, Mario H. Yánez-Muñoz, Miguel T. Rodrigues, Roberta Graboski, Fabio A. Machado, Marco Altamirano-Benavides, Sandro L. Bonatto & Felipe G. Grazziotin

View supplementary material

Published online: 22 Aug 2018.

Submit your article to this journal

View Crossmark data

Taylor & Francis
Taylor & Francis Group

Check for updates

Research Article

Origin and hidden diversity within the poorly known Galápagos snake radiation (Serpentes: Dipsadidae)

HUSSAM ZAHER[1] (iD), MARIO H. YÁNEZ-MUÑOZ[2] (iD), MIGUEL T. RODRIGUES[3] (iD),
ROBERTA GRABOSKI[1] (iD), FABIO A. MACHADO[4] (iD), MARCO ALTAMIRANO-BENAVIDES[5,6] (iD),
SANDRO L. BONATTO[7] (iD) AND FELIPE G. GRAZZIOTIN[8] (iD)

[1]Museu de Zoologia, Universidade de São Paulo, Avenida Nazaré 481, Ipiranga, São Paulo, SP, 04263-000, Brazil;
[2]Instituto Nacional de Biodiversidad, Av. De los Shyris y Rumipamba 341, Quito, Ecuador;
[3]Instituto de Biociências, Universidade de São Paulo, Rua do Matão, Travessa 14, Cidade Universitária, São Paulo, SP,
05508-900, Brazil;
[4]División de Mastozoología, Museo Argentino de Ciencias Naturales "Bernardino Rivadavia" CONICET, Av. Ángel Gallardo 470,
Buenos Aires (C1405DJR), Argentina;
[5]Instituto de Investigaciones Cientificas y Tecnológicas (INCYT), Universidad Iberoamericana del Ecuador, 9 de Octubre N25-12 y
Colón, Quito, Ecuador;
[6]Estación Científica Amazonica Juri-Juri Kawsay, Universidad Central del Ecuador, Av. América N23-41 y Mercadillo,
Quito, Ecuador;
[7]Laboratório de Biologia Genômica e Molecular, Pontifícia Universidade Católica do Rio Grande do Sul, Av. Ipiranga 6681,
90619–900, Porto Alegre, RS, Brasil;
[8]Laboratório de Coleções Zoológicas, Instituto Butantan, Av. Vital Brasil, 1500, Butantã, São Paulo, SP, 05503-900, Brazil

Galápagos snakes are among the least studied terrestrial vertebrates of the Archipelago. Here, we provide a phylogenetic analysis and a time calibrated tree for the group, based on a sampling of the major populations known to occur in the Archipelago. Our study revealed the presence of two previously unknown species from Santiago and Rábida Islands, and one from Tortuga, Isabela, and Fernandina. We also recognize six additional species of *Pseudalsophis* in the Galápagos Archipelago (*Pseudalsophis biserialis* from San Cristobal, Floreana and adjacent islets; *Pseudalsophis hoodensis* from Española and adjacent islets; *Pseudalsophis dorsalis* from Santa Cruz, Baltra, Santa Fé, and adjacent islets; *Pseudalsophis occidentalis* from Fernandina, Isabela, and Tortuga; *Pseudalsophis slevini* from Pinzon, and *Pseudalsophis steindachneri* from Baltra, Santa Cruz and adjacent islets). Our time calibrated tree suggests that the genus *Pseudalsophis* colonized the Galápagos Archipelago through a single event of oceanic dispersal from the coast of South America that occurred at approximately between 6.9 Ma and 4.4 Ma, near the Miocene/Pliocene boundary. www.zoobank.org/urn:lsid:zoobank.org:pub:2679FD19-01E5-48FE-A0DA-A88FF145DE56

Key words: Dipsadidae; divergence time estimation; island speciation; molecular phylogeny; Pseudalsophis; Serpentes

Introduction

Despite more than 200 years of intensive research in the Galápagos islands, only a few systematic and ecological studies, notably Van Denburgh (1912) and Thomas (1997), have been published on snakes, leading to only preliminary taxonomic and biogeographic conclusions (Slevin, 1935; Thomas, 1997; Zaher, 1999) mostly through the analysis of old museum specimens. As a result, very little is known about their ecology, natural history, and conservation status.

Snakes are very specific and unique predators within the reptile community of the Galápagos Islands, and it is expected that their direct and indirect interactions can significantly alter and model the community structure of vertebrates and invertebrates of these islands. Known prey include insects (grasshoppers, beetles, moths), intertidal rock marine fish (e.g., four-eyed blenny), lizards (lava-lizards, geckos, hatchling marine iguanas), birds (hatchling cucuves), and small mammals (endemic rice rats) (Beebe, 1924; Merlen & Thomas, 2013; Van Denburgh, 1912).

Correspondence to: Hussam Zaher. E-mail: hussam.zaher@gmail.com

In general, endemic snakes from oceanic or island eco-systems are particularly vulnerable/endangered, but before any monitoring, conservation, or management programmes can be developed, it is critical to determine the taxonomic status of the Galápagos snakes, the phylogeographic structure of their recognizable populations, and their phylogenetic affinities within the New World dipsadid radiation of snakes (Grazziotin et al., 2012; Zaher et al., 2009).

The lack of previous thorough systematic treatment of Galápagos snakes is understandable given that most specimens in scientific collections are unsuitable for anatomical studies or DNA extraction due to their rarity or their preservation. As such, the Galápagos snake radiation remains one of the poorest known groups of terrestrial vertebrates in the Archipelago. In order to obtain new samples that would allow a more detailed phylogenetic and taxonomic analysis of the group, we conducted in June 2008 a joint expedition of the Museum of Zoology of the University of São Paulo (MZUSP) and Instituto Nacional de Biodiversidad (INABIO) (former Museo Ecuatoriano de Ciencias Naturales, MECN) that visited 14 islands and islets of the Archipelago in 15 days (Fig. S1, see online supplemental material, which is available from the article's Taylor & Francis Online page at https://doi.org/10.1080/14772000.2018.1478910). Our new sampling represents an important addition to the limited number of specimens of Galápagos snakes already preserved in museums worldwide and helps to fill a significant gap in our knowledge of the group.

According to Zaher (1999), the Galápagos snakes are a monophyletic group that is most closely related to the mainland South American '*Alsophis*' *elegans* and *Saphenophis*, without any special affinities to any of the West Indian genera (Thomas, 1997). Subsequently, Zaher et al. (2009) erected the new genus *Pseudalsophis* to accommodate the mainland *Alsophis elegans* and the Galápagos species, allocating both genera *Pseudalsophis* and *Saphenophis* in the tribe Saphenophiini. However, the phylogenetic affinities and taxonomic status of the Galápagos snakes remain unsolved. Additionally, the phylogeographic structure of their populations along all 13 major Galápagos Islands and their satellites also remain virtually unexplored.

Here, we provide a phylogenetic analysis of the Galápagos snake radiation that includes most populations known to occur in the Archipelago. We describe three new species for genus *Pseudalsophis* and test its monophyly with the largest sampling of dipsadid species so far. We also provide a time calibrated tree and discuss the origin, radiation, and phenotypic evolution of the species of snakes in the Archipelago.

Materials and methods
Specimens examined, meristic counts, and measurements

We examined and compared 322 specimens of *Pseudalsophis* (Table S1, see supplemental material online) deposited in the following institutions (acronyms used in the text are given in parentheses): Museu de Zoologia da Universidade de São Paulo (MZUSP); National Museum of Natural History, Washington (USNM); American Museum of Natural History, New York (AMNH); Instituto Nacional de Biodiversidad, Quito (DHMECN); Museum of Vertebrate Zoology at Berkeley (MVZ); Natural History Museum, London (BMNH); California Academy of Sciences, San Francisco (CAS); Muséum National d'Histoire Naturelle de Paris (MNHN); Field Museum of Natural History, Chicago (FMNH); Academy of Natural Sciences, Philadelphia (ANSP); San Diego Natural History Museum (SDNHM); Museo de Vertebrados, Fundación Charler Darwin, Puerto Ayora (CDRS and MVECCD); Peabody Museum of Natural History, Yale University, New Haven (YPM); Senckenberg Forschungsinstitut und Naturmuseum, Frankfurt am Main (SMF). Total length (TTL), snout–vent length (SVL), and tail length (TL) were measured to the nearest 1 mm by carefully stretching the specimens along a ruler. Snout length (SL), head length (HL) and head scale length were measured to the nearest 0.1 mm with a digital calliper. HL was measured from the tip of the rostral to the retroarticular process of the lower jaw. SL was measured from the tip of the rostral to the anterior edge of the eye. Head scales were measured only on the right side of the specimen. Most measures were converted to proportions for purposes of description. Images were taken with a digital camera and mounted in plates with the aid of Adobe Photoshop. Ventral scales were counted beginning from the first preventral scale. However, preventral numbers are given in parentheses to facilitate comparisons with counts from other authors that begin from the first ventral scale distinctly wider than long (Dowling, 1951; Myers, 2003). Dorsal scales were counted in three distinct places in the body, at the level of the first ventral scales, at mid-body, and five to eight dorsal scale rows prior to the cloaca. Divided subcaudal scales were counted on only one side, from the first pair posterior to the cloaca that touches medially to the last undivided (terminal shield) scale.

Itinerary of the expedition, field procedures, and hemipenial preparations

Our joint INABIO-MZUSP expedition to the Galápagos Archipelago visited 14 islands and islets in a period of

15 days (Fig. S1). The itinerary was arranged with the Direction of Parque Nacional Galápagos who provided the collecting permit number 060-2008 (Project PC-17-07) for the islands of Santa Cruz, Santa Fé, Española, San Cristóbal, Floreana, Tortuga, Isabela, Fernandina, Santiago, Rábida, Pinzón, and adjacent islets (e.g., Gardner near Española, Gardner near Floreana, Champion, and Sombrero Chino).

We did not survey the following islands and islets where snake populations may well be present but were not registered so far: Quatro Hermanos and Redonda Islets, located on the north-western and south-eastern portions of Isabela Island; Bartolomé, Bainbridge, Albany, Beagle, and Tiburon islets near Santiago Island; Daphne Maior, Plaza Sur, Eden, and Guy Fawkes islets near Santa Cruz Island; Enderby, Watson, and Caldwell near Floreana Island. Snakes were never recorded in the northern islands of Darwin (Culpepper), Wolf (Wenman), Pinta (Adington), Marchena (Bindloes), and Genovesa (Tower).

We collected a total of 86 live specimens from which 39 were sacrificed for osteological and hemipenial preparation and 47 were sampled and released. One species (*P. occidentalis* from Fernandina Island) dominated the sampling (44 specimens), with samples from other populations varying from one to five individuals. We extracted tissue samples from all live individuals that were collected by clipping the tip of 5 ventral scales. All tissue samples were preserved in ethanol 96%.

Sex was determined in live specimens by everting partially the hemipenis at the base of the tail. Both hemipenes of freshly killed male specimens were removed and prepared separately prior to formaldehyde preservation of the whole specimen. Special attention was given during these preparations to fully evert the lobes and expand the hemipenis to its maximum capacity (Myers & Cadle, 2003). Eversion was facilitated by cutting the retractor muscles away from the tip of their inverted lobes and manually separating the latter (Zaher & Prudente, 2003). Further hemipenial preparation and terminology followed Zaher (1999), Myers and Cadle (2003), and Zaher and Prudente (2003).

Taxon sampling for DNA sequencing

We generated sequence data for a total of 34 *Pseudalsophis* individuals, two from mainland Peru and 32 from the Galápagos Archipelago. Sample sizes for species and islands varied substantially and we used up to three individuals per island in order to equalize our sampling with at least one individual representing each known insular population sampled during the expedition. We were unsuccessful in collecting tissue samples from

populations known to occur in some of the islets off Santiago and Santa Cruz, and from populations of *P.* cf. *slevini* in Fernandina, *P. biserialis* in Floreana (and adjacent islets), and *P.* cf. *steindachneri* in Rábida. On the other hand, we successfully extracted DNA from three shed skins found in the field, two from individuals of *P. dorsalis* from Seymour Norte and one from an individual of *P. hoodensis* from Española. Shed skins were identified based on scale counts, individual size, and the pattern of species distribution throughout the islands. The two skin samples from Seymour Norte corresponded in our analysis to the only individuals of *P. dorsalis* from the closely connected islands of Santa Cruz, Baltra, and Seymour Norte since no live specimens of *P. dorsalis* were found in these three islands during our expedition (Fig. S1, see supplemental material online). The skin from Española usefully augmented our sampling of *P. hoodensis* with only one specimen collected on this island (a list of species and loci sequenced are provided in Table S2 (see supplemental material online).

DNA sequencing

We extracted DNA from scales, muscles, and shed skins using the PureLink® Genomic DNA kit (ThermoFisher, MA, USA). Sequence fragments for six genes were amplified via polymerase chain reaction (PCR) using the following pairs of primers: for 12S, 16S, and c-mos, we used the set of primers as described in Zaher et al. (2009); for cytb, we used the primers described by Grazziotin et al. (2012); for bdnf and nt3, we used the primers described by Noonan and Chippindale (2006). PCRs were performed using standard protocols, with adjustments to increase the efficiency of amplification as following: addition of 10% of Trehalose 100 for 12S, 16S, and cytb; and 0.4% of Triton 100 for bdnf and nt3.

We used an annealing temperature of $54\,^{\circ}C$ for 12S and 16S, $56\,^{\circ}C$ for bdnf, a touchdown cycle of $60{-}50\,^{\circ}C$ with final annealing of $54\,^{\circ}C$ for cytb and c-mos. PCR products were purified with shrimp alkaline phosphatase and exonuclease I (GE healthcare, Piscataway, NJ), and the sequences were processed using the DYEnamic ET Dye Terminator Cycle Sequencing Kit in a MegaBACE 1000 automated sequencer (GE Healthcare) following manufacturer's protocols. Both strands were checked, and when necessary edited manually. The consensus of both strands was generated using Geneious 7.1.8 (http://www.geneious.com; Kearse et al., 2012).

Molecular analyses

The affinities of *Pseudalsophis* and monophyly of Saphenophiini were tested with an extended data set for

the family Dipsadidae that included six genes (total alignment length of 3,938 base pairs) and 344 taxa (matrix available at Dryad Digital Repository database: http://dx.doi.org/10.5061/dryad.18cg032). This data set is the basis for the most comprehensive assessment of dipsadid phylogenetic relationships currently available, including 36% of all species and 87% of all genera known so far, and was designed to incorporate the largest number of sequences of Dipsadidae available in GenBank. To check for misidentified, mislabelled, or misassembled sequences of Dipsadidae deposited in GenBank we estimated gene trees through Maximum likelihood (ML) phylogenetic analysis using the same parameters set for the analyses of the complete data set (see below). We avoided using sequences for terminals that did not group consistently with their families. We also added to this data set new sequences from 95 species representing 38 dipsadid genera, including one specimen of *Saphenophis antioquiensis*, totalling 277 dipsadid species, but included only one individual for each species of *Pseudalsophis* recognized in this study. Alternatively, the data matrix used to test the relationships among species and populations of *Pseudalsophis* included six genes (total alignment length of 3,878 base pairs) and only 99 terminals (matrix available at Dryad Digital Repository database: http://dx.doi.org/10.5061/dryad.18cg032). This second data set was designed to reduce outgroup sampling (65 terminal taxa), but included all the sequence data generated for *Pseudalsophis* (34 individuals) in this study. Complete lists of terminals, sampled genes, and accession numbers of the two data sets used in our analyses are provided in Table S2 (see supplemental material online).

Sequences were aligned using MAFFT 1.3.6 (Katoh, Kuma, Toh & Miyata, 2005) as implemented in Geneious 7.1.8. Both 12S and 16S genes were aligned by applying the E-INS-i algorithm, while coding genes were aligned under the G-INS-i algorithm. We used default parameters for gap opening and extension. All protein-coding genes were visually checked using Geneious to verify the correct reading frame.

We used PartitionFinder 2 (Lanfear, Frandsen, Wright, Senfeld, & Calcott, 2016) to choose the combined sets of partitioning schemes and models of molecular evolution based on the Akaike Information Criterion with correction (AICc). We treated the two rRNA genes as separate partitions and partitioned protein coding genes by codon positions. We used the greedy search option in PartitionFinder, allowing only the selection of models of molecular evolution implemented in RAxML 8.2.3 (Stamatakis, 2014) without any correction for proportion of invariant sites, as recommended in the RAxML's manual. We performed ML

analyses using RAxML 8.2.3, conducting a rapid bootstrap analysis (1,000 replicates) and search for the best scoring ML tree (estimated 200 times using as starting tree every 5th bootstrap tree) in the same run (option -f a).

Divergence time estimation

We estimated divergence times among lineages using a Bayesian approach implemented in BEAST v2.4.7 (Bouckaert et al., 2014), with our second data set reduced to include only two individuals of *Pseudalsophis* per island in order to match our data with the selected tree prior for speciation. We also pruned several outgroup terminals, keeping only a representative diversity of dipsadids with terminals that were essential for setting calibration points. Pruning resulted in a reduced data set with six genes (3,878 base pairs) for 28 *Pseudalsophis* and 39 outgroups (matrix available at Dryad Digital Repository database: http://dx.doi.org/10.5061/dryad.18cg032). We set the data partitions as defined by Bayesian Information Criterion in PartitionFinder and we ran the analyses with bModelTest (Bouckaert & Drummond, 2017) as site model, allowing BEAST to average over all models. When implemented, bModelTest switches between substitution models during the MCMC analysis, inferring and marginalizing site models, thus averaging out uncertainty over such models. The mutation rate was estimated for all partitions and the set of models was defined as 'allreversible'. We also ran BEAST with bModelTest on the partition set defined by loci (mtDNA and three nuclear genes), aiming to compare and explore both approaches. We used the partitions as defined by PartitionFinder because bModelTest does not incorporate averaging site models over partitions from the alignment (Bouckaert & Drummond, 2017).

We set the prior for the clock model as Relaxed Clock Log Normal and the tree prior was set to Yule Model. Five calibration points (enforcing monophyly) were set with Log Normal distributions with mean 1.0 and standard deviation of 1.25, as follows: (1) stem Caenophidia, offset in 54 Ma (95% quantile in 75.2 Ma); (2) stem Crotalinae, offset in 10.3 Ma (95% quantile 24.4 Ma); (3) stem New World Dipsadidae, offset in 12.5 Ma (95% quantile 26.6 Ma); (4) stem Elapidae, offset in 24.9 Ma (95% quantile 46.1 Ma); and (5) crown Natricidae, offset in 13.8 Ma (95% quantile 35.0 Ma). The description of each fossil used and rationale for each calibration point are given in Table S3 (see supplemental material online). We also defined three other monophyletic taxon sets in order to improve the initial likelihood, as suggested by the RAxML tree topology. The monophyletic taxon sets were: Endoglyptodonta, the Galápagos radiation, and the clade

formed by Pseudoxenodontidae and Dipsadidae. We ran three independent runs (different seeds) with 50 million generations, sampling each 1,000 generation.

We used Tracer v1.6.1 (Rambaut, Suchard, Xie, & Drummond, 2014) to check for trace convergence and values of ESS (effective sample size), and LogCombiner v2.4.7 (Bouckaert et al., 2014) to perform the burn-in and subsample the tree files to 10,000 trees. TreeAnnotator v2.4.7 (Bouckaert et al., 2014) was used to summarize the tree distribution and the estimated parameters.

Haplotype network

We evaluated the relationship among some recent populations of *Pseudalsophis* using cytb sequences in a haplotype network analysis through the *R* packages *haplotypes* (Aktas, 2015), *network* (Butts, 2015), and *sna* (Butts, 2016).

Morphometric analyses

We used five measured characters in a total of 322 individuals for our morphometric analyses (120 females, 161 males, 41 undefined): SVL, TL, HL, ventral, and subcaudal counts. Outliers were evaluated through visual inspection of histograms and bivariate plots against SVL (Zuur, Ieno, & Elphick, 2010). We calculated mean, standard deviations, maximums, and minimums of the variables for all taxa and sexes.

Normality was investigated through visual inspection of Quantile-Quantile plots (which also helps in the identification of outliers) and through Lilliefors (Kolmogorov–Smirnov) tests with a Bonferroni correction for multiple tests. If all taxa were evaluated, 7% of the tests rejected the null hypothesis of normality. However, if we group different populations of the same species (as suggested by results), no test rejected the null hypothesis. Additionally, if we perform the tests on the full polled mean-cantered data, we fail to reject the null hypothesis in all cases. Even though scale counts are not continuous data *per se*, for snakes they are thought to vary in an almost continuous manner and are routinely modelled using normal distributions in evolutionary studies (e.g., Arnold & Phillips, 1999; Lindell, 1994; Phillips & Arnold, 1999). For that reason, we analysed count data along with linear measurements. Given that metric traits are expected to strongly co-vary due to body size, HL and TL were graphically evaluated as ratios in relation to SVL and total length (TTL = SVL + TL), respectively.

Sexual dimorphism was evaluated for all characters through t-tests with Bonferroni P-corrections for multiple tests within each species. To investigate differences between taxa we performed analyses of variance (ANOVA) and a *post-hoc* Tukey all-pairs comparison on each individual character for both sexes separately and for the full pooled sample. Because differences in allometric scaling can lead to false conclusions while using ratios for morphometric analysis (e.g., Molina, Machado, & Zaher, 2012) we conducted analyses of covariance (ANCOVAS) on both HL and TL on the logarithmic scale using taxon as factor and log(SVL) as a covariate.

We investigated the multivariate difference between taxa performing a Linear Discriminant Analysis (LDA) with a subset of specimens containing no missing data (143 specimens; 60 females, 83 males). LDA is a multivariate technique that evaluates the capacity of the morphometric data to correctly assign a specimen to its *a priori* group by extracting axes (or functions) that maximize the between-group variation while taking within-group variation into account. Given that some level of sexual dimorphism was identified (Table S4; see supplemental material online), differences between sexes were corrected for through the use of a linear model using sex as a factor. Residuals of the model were added to the mean values of the female of each species, thus removing sex differences. Posterior classifications were calculated for the full sample and through a leave-one-out cross-validation procedure in order to estimate multivariate superposition between groups (Carvalho et al., 2016; Machado & Hingst-Zaher, 2009; Silva, de Oliveira, Nascimento, Machado, & Prudente, 2017). *Pseudalsophis elegans* was excluded from this step of the analysis due to lack of morphometric data. LD functions calculated for the full sample were used to visualize the multivariate ordination of the data. Additionally, the Euclidian distance between all individuals on the LD axis (which is equivalent to the Mahalanobis distance) was obtained and submitted to a Ward clustering method, an agglomerative hierarchical clustering procedure that minimizes the within-cluster dissimilarities and produces spherical clusters on a multivariate space.

We estimated ancestral character states for each trait by ML on the time calibrated tree (Schluter, Price, Mooers, & Ludwig, 1997). Resulting hypothetical ancestral states were projected onto the LD functions in order to describe overall patterns of phenotypic evolution. Hypothetical ancestors were classified as belonging to the clusters found on Ward clustering by summing the posterior probabilities of belonging to any of the species on a given cluster.

Lastly, because of the results from molecular, univariate, and multivariate morphometric analysis and the lack of clear diagnostic features (see below), *P. biserialis* from Floreana and San Cristóbal Islands, and *P. occidentalis* from Fernandina, Tortuga, and Isabela Islands were clustered together in order to produce the species summary statistics.

Results

Partitions and models of evolution
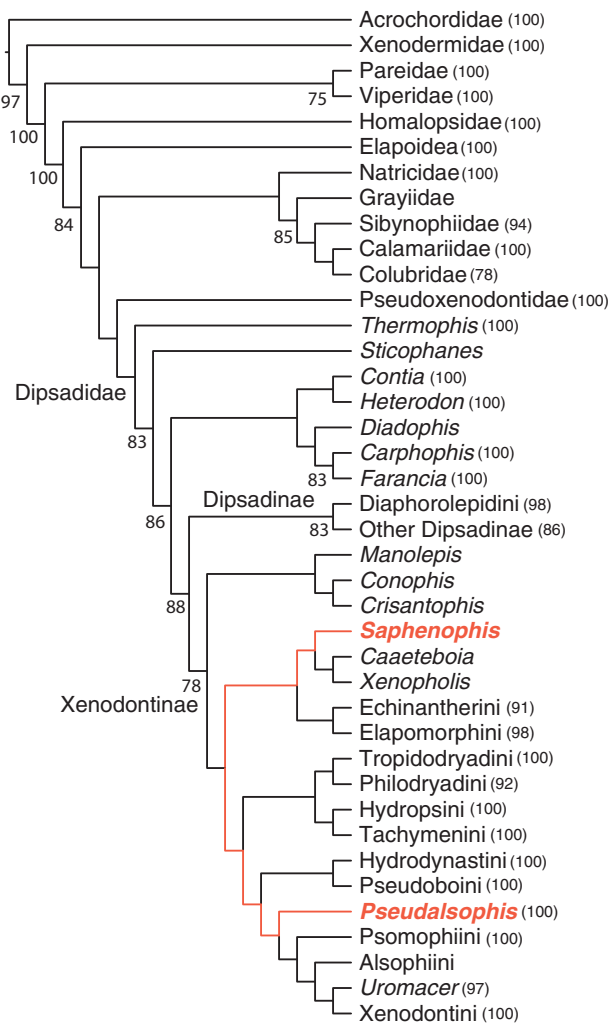
The best partition scheme selected for the extended dipsadids data set combined the initial 14 matrix partitions in three composed partitions: (1) both rRNAs, and the 1st and 2nd positions of cytb; (2) only cytb's 3rd position; and (3) all three nuclear genes. The selected site model for all three partitions was $GTR + G$. The estimated best partition scheme and site models using BIC were the same as selected for the extended dipsadid data set.

Higher-level phylogenetic affinities within Dipsadidae

The tree topology from our extended ML data set analysis (Fig. 1; Fig. S2, see supplemental material online)

recovered the monophyletic superfamilies Colubroidea and Elapoidea (*sensu* Zaher et al., 2009) with maximal bootstrap support. Among caenophidian families Acrochordidae, Xenodermidae, Pareidae, Viperidae, Homalopsidae, Lamprophiidae, Pseudoxyrhophiidae, Elapidae, Natricidae, and Pseudoxenodontidae all have maximal bootstrap support. Atractaspididae (96%), Psammophiidae (83%), and Sibynophiidae (94%) have strong support (values in parentheses), and only Colubridae and Dipsadidae were not recovered with strong bootstrap support.

Within Dipsadidae, the Asiatic genera *Thermophis* and *Stichophanes* were retrieved as successive sister groups of the remaining Dipsadidae, and subfamilies Dipsadinae and Xenodontinae were recovered as monophyletic, but with low bootstrap support. *Stichophanes* and all other dipsadid taxa, except *Thermophis*, formed

Figure 1. Summary tree of our extended ML analysis (Fig. S2, see supplemental material online). The tree indicates the deep-level relationships among suprageneric taxa of Colubroides, tribes of Dipsadidae and genera of Xenodontinae. Branches linking the genera *Saphenophis* and *Pseudalsophis* are highlighted in red. Numbers are bootstrap proportions. Bootstrap values less than 70% are not shown.

a strongly supported clade (83%). The subfamily Carphophiinae was retrieved as non-monophyletic in our tree, with *Heterodon* and *Farancia* nested inside it as sister-groups of *Contia* (<70%) and *Carphophis* (83%), respectively. However, this larger North American 'relictual' clade has low support (<70%).

Our analyses recovered the following tribes of Dipsadidae as monophyletic: Diaphorolepidini (98%); Imantodini (94%); Dipsadini (74%); Conophiini (<70%); Echinantherini (91%); Elapomorphini (98%); Tropidodryadini (100%); Philodryadini (92%); Hydropsini (100%); Tachymenini (100%), Hydrodynastini (100%), Pseudoboini (100%), Psomophiini (100%), Alsophiini (*sensu* Grazziotin et al., 2012; <70%), and Xenodontini (100%). The tribe Saphenophiini (Zaher et al., 2009) was expected but not retrieved as monophyletic, with *Pseudalsophis* positioned as the sister group of a clade including Xenodontini, Alsophiini, and Psomophiini, whereas *Saphenophis* grouped in a clade otherwise composed of *Caaeteboia* and *Xenopholis* (Fig. 1; Fig. S2, see supplemental material online). Both clades received low (<70%) bootstrap support.

Phylogenetic affinities of the Galápagos snakes

The genus *Pseudalsophis* is monophyletic in both extended (Fig. 1; Fig. S2, see supplemental material online) and reduced ML analyses (Fig. 2; Fig. S3, see supplemental material online), with unequivocal, maximal bootstrap support. We also recovered the same pattern of cladogenesis within *Pseudalsophis* in both ML analyses, except that the nodes received higher bootstrap support in the ML tree derived from the reduced data set (Fig. 2; Fig. S3, see supplemental material online).
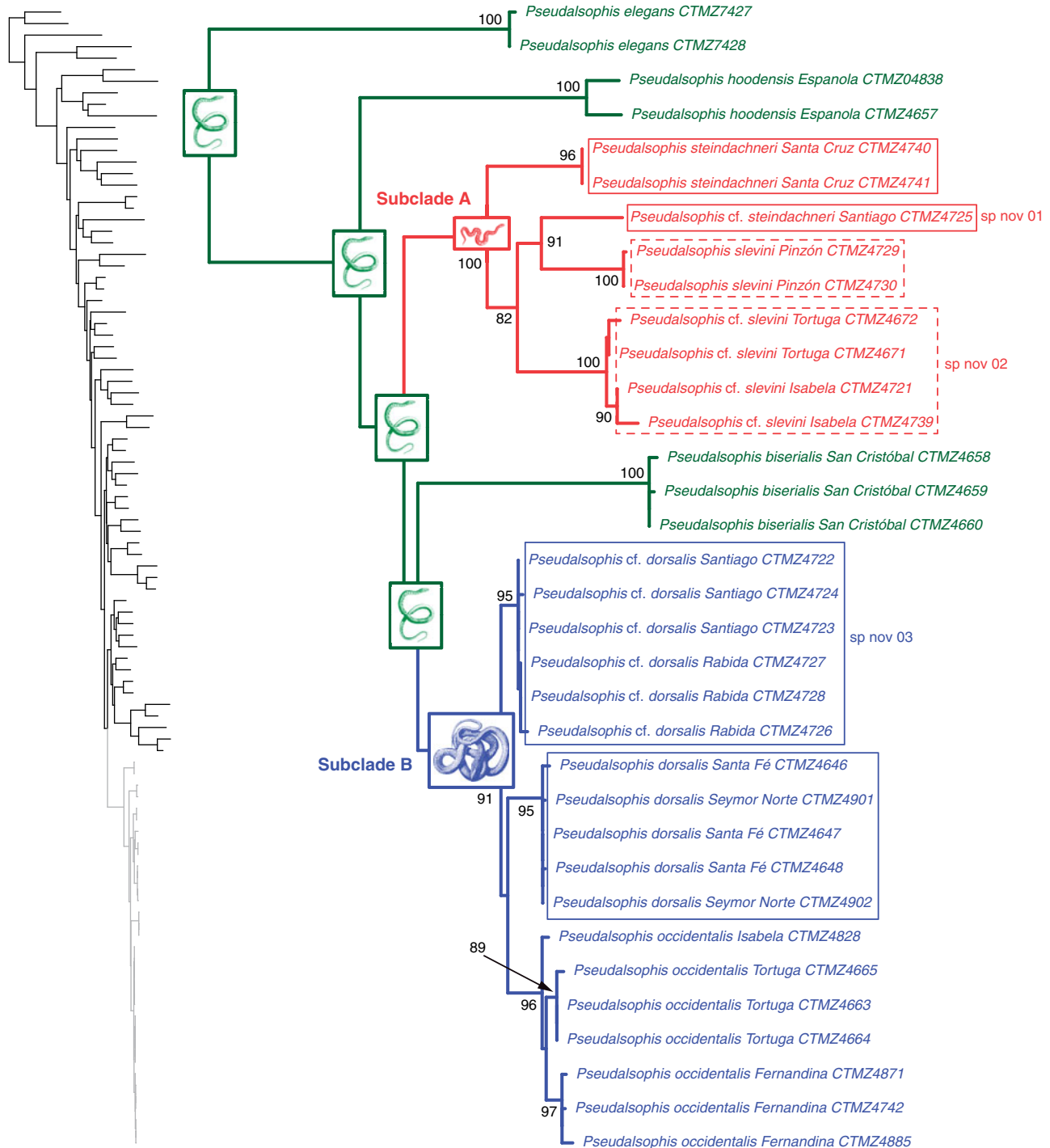
The mainland *Pseudalsophis elegans* is the sister-group of the Galápagos radiation of snakes in both analyses, but strongly supported (82%) by bootstrap values only in the extended ML analysis (Fig. S2, see supplemental material online). Within the Galápagos clade, *P. hoodensis* was retrieved as the sister group of a clade that includes *P. biserialis* and two strongly supported subclades, one formed by the small insular species *P. slevini* and *P. steindachneri* (subclade A, 89%), and the other composed by the large insular species *P. dorsalis* and *P. occidentalis* (subclade B, 99%). *Pseudalsophis slevini*, *P. steindachneri*, and *P. dorsalis* are non-monophyletic species in the extended ML analysis, despite the reduced number of *Pseudalsophis* terminals included in this dataset.

The ML tree derived from our reduced analysis (Fig. 2) also recovered the two well-supported subclades A and B (formed by *P. slevini* and *P. steindachneri*, and *P. dorsalis* and *P. occidentalis*, respectively) and
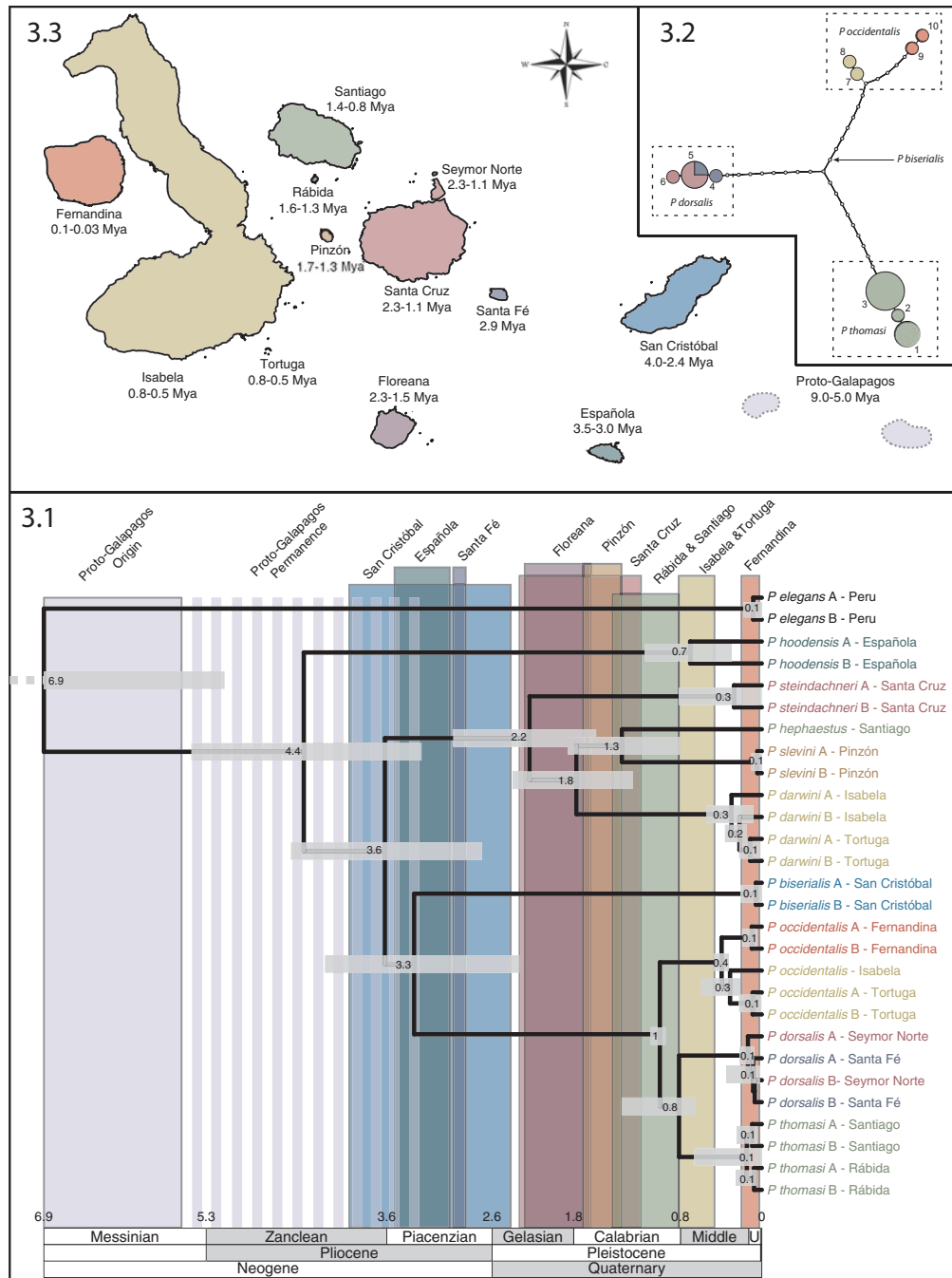
confirmed non-monophyly of the three traditionally recognized Galápagos species *P. steindachneri*, *P. slevini*, and *P. dorsalis*. Subclades A and B were maximally or strongly (91%) supported, respectively. Within subclade A, individuals of *P. steindachneri* from Santa Cruz Island are the sister group of a well-supported clade (82%) composed by the only sampled individual of *P.* cf. *steindachneri* from Santiago Island and all individuals of *P. slevini*. This clade also indicates that individuals of *P. slevini* from Pinzón Island share a closer ancestor with *P.* cf. *steindachneri* from Santiago Island (91%) than with the population of *P.* cf. *slevini* from Tortuga and Isabela Islands. The non-monophyletic condition of these two species within subclade A is highlighted in Fig. 2. Within subclade B, individuals of *P. dorsalis* from Santa Fé and Seymour Norte Islands did not cluster together with individuals of *P.* cf. *dorsalis* from Santiago and Rábida Islands. Instead, individuals from Santa Fé/Seymour Norte form a weakly supported clade with individuals of *P. occidentalis* from Isabela, Tortuga, and Fernandina Islands. The two distinct lineages of *P. dorsalis* and *P.* cf. *dorsalis* are indicated in the ML tree with two solid blue boxes (Fig. 2). The paraphyletic condition of *P. dorsalis* shown in our ML tree (Fig. 2) was not replicated in the BEAST analysis (Fig. 3.1; Fig. S4, see supplemental material online) where populations of *P. dorsalis* from Santa Fé/ Seymour Norte and *P.* cf. *dorsalis* from Santiago/ Rábida formed two distinct sister-clades (Fig. 3.1; Fig. S4, see supplemental material online).

Meristic and morphometric comparisons

Based on our phylogenetic results, geographic distribution, and external morphology, Galápagos snakes were divided into 11 different groups for statistical analysis: *P. hoodensis*, *P. biserialis* from Floreana Island, *P. biserialis* from San Cristóbal Island, *P. occidentalis* from Fernandina Island, *P. occidentalis* from Tortuga and Isabela Islands, *P. dorsalis*, *P.* cf. *dorsalis* from Santiago and Rábida Islands, *P. steindachneri*, *P.* cf. *steindachneri* from Santiago Island, *P. slevini*, and *P.* cf. *slevini* from Tortuga and Isabela Islands. T-tests detected 11 instances of significant sexual dimorphism (Table S4; see supplemental material online). *Pseudalsophis hoodensis* was the most dimorphic species, having females with larger SVL, smaller proportional tails (TL/TTL) and fewer subcaudals. *Pseudalsophis biserialis* from San Cristóbal and *P. steindachneri* also presented females with proportionally small tails with fewer subcaudals. Both *P. occidentalis* from Fernandina and *P. dorsalis* had females with more ventrals than males. *Pseudalsophis dorsalis* also had

Figure 2. ML tree estimated using the reduced matrix showing the relationships within *Pseudalsophis*. The topology of the complete ML tree is provided on the left; the area highlighted in grey corresponds to the *Pseudalsophis* radiation (Fig. S3, see supplementary material online). Numbers are bootstrap proportions. Bootstrap values less than 70% are not shown. Branches and tip labels are coloured as to indicate the optimization of the morphotypes (green, continental morphotype; red, small insular morphotype; and blue, large insular morphotype). Solid blue boxes indicate the two distinct lineages of *P. dorsalis* and *P.* cf. *dorsalis*; solid red boxes show both lineages of *P. steindachneri* and *P.* cf. *steindachneri*; dashed red boxes indicate the lineages of *P. slevini* and *P.* cf. *slevini*.

Figure 3. Calibrated Bayesian tree for the *Pseudalsophis* radiation (3.1), haplotype network for the 'large insular morphotype' group of species (3.2), and map of the Galápagos Archipelago showing approximate island ages (3.3). Values below the island names represent the maximum age estimated by the Nazca plate movement (first value) and by lava exposure age determination (second value). Each island is coloured based on its estimated age of emergence (3.3). The same colours are used in the boxes representing the age range of emergence for each island in the calibrated tree (3.1). The taxon names in the tree and the haplotype network circles also received the same colours, representing the species and the haplotype distributions in the archipelago. The indicated location of the Proto-Galápagos Islands corresponds to an approximation based on recent literature (see text) and does not represent a precise estimation. The estimated age range for the origin of the Proto-Galápagos Islands is represented with a solid grey box (3.1), and its grey hachured area represents the estimated permanence of these islands as dry aerial land masses before subsidence. Values near the nodes of the calibrated tree indicate the estimated age in millions of years, and the grey bars represent the confidence interval for each age. The small white circles on the haplotype network indicate estimated missing intermediates; the numbers near the circles indicate the haplotype code (see Table S2, see supplemental material online). The relative size of circles represents the frequency of each haplotype.

females with smaller tails, and *P.* cf. *steindachneri* had females with less ventrals than males.

All ANOVAS used to differentiate between taxonomic units were significant (P value <0.05), both for the pooled sample and for each sex analysed separately. The pairwise *post-hoc* Tukey tests reveals a complex pattern of morphometric differentiation among Galápagos snakes (Table S5; see supplemental material online), that can be summarized as follows. For body size (Fig. S5, see supplemental material online) there is a main differentiation between larger taxa (*P. occidentalis*, *P. dorsalis*, and *P.* cf. *dorsalis*) and smaller taxa (*P. steindachneri*, *P.* cf. *steindachneri*, *P slevini*, and *P.* cf. *slevini*). *Pseudalsophis occidentalis* from Fernandina is the largest taxon, differentiating itself from almost all other taxa, with the exception of *P. occidentalis* from Isabela and Tortuga. For *P. hoodensis*, due to sexual dimorphism, females, but not males, are distinct from the small taxa.

For relative tail-length (TL/TLL; Fig. S5.1, see supplemental material online) there are broadly two groups: one formed by species with a proportionally large tail, including *P. elegans*, *P. biserialis*, *P. steindachneri*, *P.* cf. *steindachneri*, *P slevini*, and *P.* cf. *slevini* and another group formed by small-tailed species, including *P. occidentalis*, *P. dorsalis*, and *P.*cf. *dorsalis* (sp. nov). *Pseudalsophis hoodensis* falls somewhat in between these two groups, having an intermediate tail-size. For relative head-length (HL/SVL; Fig. S5.2, see supplemental material online) differentiation is less clear, with *P. elegans*, *P.* cf. *biserialis*, *P.* cf. *steindachneri*, *P. slevini* and *P.* cf. *slevini* showing proportionally larger heads then the rest of the species.

The allometric analysis of TL and HL shows a significant effect of SVL on both variables, as well as an effect for taxa and the interaction between taxa and SVL, suggesting that species differ in allometric relationships. Inspection of bi-logarithmic plots (Fig. S6, see supplemental material online) suggests that the main difference lies in the contrast between large-bodied taxa and small-bodied taxa (as defined for SVL above). In fact, the exclusion of small-bodied taxa produced nonsignificant interaction terms for both variables, suggesting a common allometric relationship among large taxa. The exclusion of large-bodied taxa produced non-significant interaction terms only for TL, while the HL still showed a significant SVL:taxa interaction. This suggests that allometric relations between HL and SVL might vary between smaller species.

Ventral counts were very conserved within species and incredibly disparate among species, leading to an almost perfect discrimination of taxa (Fig. S7, see supplemental material online). The only exceptions were the comparison among *P.* cf. *steindachneri*, and *P.* cf. *slevini*, between both *P. occidentalis* populations, among *P. hoodensis* and *P.* cf. *biserialis*, and among *P. elegans* and *P. hoodensis*, *P. biserialis* (Floriana) and *P.* cf. *dorsalis*. Additionally, there is a clear pattern among ventral counts with the formation of three groups: one containing *P. elegans*, *P. hoodensis*, and *P.* cf. *biserialis* that shows intermediary values (200–220), a second one composed of *P.* cf. *occidentalis* and *P.* cf. *dorsalis* with higher values (>210), and a third one composed of *P.* cf. *steindachneri* and *P.* cf. *slevini* with lower values (<190). Subcaudal counts did not show any evident pattern of differentiation (Fig. S7, see supplemental material online) , except for the population of *P. biserialis* from San Cristóbal that showed more subcaudal scales than any other Galápagos population (especially when we take males into account), and for *P. steindachneri* and *P.* cf. *slevini* that showed fewer numbers of subcaudal scales among sampled populations.

The multivariate linear discriminant analysis showed that differentiation occurred almost entirely along a single axis (Fig. S8, see supplemental material online). The character loadings on this axis points to the negative influence of two main characters: ventral counts and head size. Correct classification rates were high overall (>80%), but with some informative exceptions (Table S6; see supplemental material online). Both populations of *P. biserialis* greatly overlapped with *P. hoodensis*; *Pseudalsophis occidentalis* from Isabela and Tortuga overlapped with both *P. dorsalis* and *P. occidentalis* from Fernandina; *P. dorsalis* showed great overlap with *P.* cf. *dorsalis*; *P.* cf. *steindachneri*, *P. slevini*, and *P.* cf. *slevini* were very similar morphometrically, with the latter species overlapping only slightly with *P. steindachneri*.

The agglomerative clustering analysis clearly separated three broadly defined morphotypes (Fig. S9, see supplemental material online): (1) a 'continental morphotype'; (2) a 'large insular morphotype', and (3) a 'small insular morphotype'. The continental morphotype consists of species that are similar to the continental *Pseudalsophis elegans*, and includes *P. hoodensis* and *P. biserialis*. These species are large in size, having proportionally large tails and proportionally small heads. For this group, ventral counts are between 200–220 and, while subcaudals show a large range of variation, most of this variation is related to sexual dimorphism in *P. hoodensis*, with males overlapping in subcaudal counts with other species of this group (100–130) and females showing significantly lower counts (<100). The large insular morphotype contains *P. dorsalis*, *P.* cf. *dorsalis*, and *P. occidentalis*. Even though this group overlaps in size with the plesiomorphic morphotype, most of the observed specimens are among the largest ones. In fact, most of the superposition between both groups is due to

Figure 4. Photographs of live specimens of the Galápagos snakes *Pseudalsophis hoodensis* from Española Island (4.1), *Pseudalsophis biserialis* from San Cristóbal Island (4.2), *Pseudalsophis occidentalis* from Fernandina Island (4.3), *Pseudalsophis dorsalis* from Santa Fé Island (4.4), *Pseudalsophis thomasi* sp. nov. yellow morph from Santiago Island (4.5), *Pseudalsophis thomasi* sp. nov. brown morph from Santiago Island (4.6), *Pseudalsophis hephaestus* sp. nov. from Santiago Island (4.7), *Pseudalsophis steindachneri* from Santa Cruz Island (4.8), *Pseudalsophis slevini* from Pinzón Island (4.9), *Pseudalsophis darwini* sp. nov. from Tortuga Island (4.10).

the extreme sexual dimorphism in *P. hoodensis*, where females are vastly larger than males. For the large insular morphotype, sexual dimorphism in size was not detected, and many of the male are as large as females. These species also present the smaller heads and tails in proportion to body size while also showing the largest ventral scale counts of all species. The small morphotype contains *P. slevini*, *P.* cf. *slevini*, *P. steindachneri*, and *P.* cf. *steindachneri*. These species are small in size, showing small counts of ventral scales (<190). Even though subcaudals counts are among the smallest, they greatly overlap with other groups. Additionally, tail length is relatively large, superposing with values observed for the continental morph. Lastly, head size is also proportionally larger for these species. Even though species of *Pseudalsophis* were restricted within one of these three morphotypes, species within clusters did not form defined mutually exclusive groups.

ML ancestral state reconstruction shows the continental morphotype to be plesiomorphic for *Pseudalsophis*, being shared not only by *P. elegans*, *P. hoodensis*, and *P. biserialis*, but by most hypothetical ancestral forms (Fig. 2). Both insular morphotypes, on the other hand, are shown to be apomorphic, each representing an independent transition from the continental morphotype.

Pattern of genetic structure among recent populations

We evaluated the genetic structure among populations using haplotype network analysis only for the clade composed by *P. occidentalis* and *P. dorsalis* (Fig. 3.2). This clade is relatively recent (<1 Ma, Fig. 3.1) and populations from each island present great overlap among meristic and morphometric data (see above). The haplotype network indicates strong genetic differentiation of populations of *P. dorsalis* from Santa Cruz and Santa Fé and of *P.* cf. *dorsalis* from Santiago and Rábida (Figs 3.2–3.3). Thirty-six mutations (from 626 bp) differentiate these two lineages, whereas *P. dorsalis* differentiate from *P. occidentalis* by only 34 mutations. Populations from Santa Fé and Santa Cruz share haplotypes, but both islands also present exclusive haplotypes for *P. dorsalis*. On the other hand, haplotypes 1 and 2 are found only in populations of *P.* cf. *dorsalis* from Santiago, while haplotype 3 is only found in Rábida.

Populations of *P. occidentalis* from Isabela and Tortuga Islands share haplotypes 7 and 8, whereas the population from Fernandina Island present two exclusive haplotypes (9 and 10) and is distinguished from the population of Isabela/Tortuga by 10 mutations (Figs 3.2–3.3).

There is no evident extant ancestral haplotype for these three lineages, since they are connected by missing intermediates (white circles in the network haplotype, Fig. 3.2). Additionally, the analysis did not position *P. biserialis* in any of the haplotypes sampled for the other three species. Notwithstanding, the branch connecting *P. biserialis* to the other species is too long for a confident estimation using haplotype network methods.

New taxonomic arrangement for the Galápagos species of *Pseudalsophis*

Our study revealed the presence of three previously undescribed species of terrestrial snakes in the Galápagos, which we formally name here. We also recognized the validity of six other distinct species – *P. hoodensis* (Fig. 4.1), *P. biserialis* (Fig. 4.2), *P. occidentalis* (Fig. 4.3), *P. dorsalis* (Fig. 4.4), *P. steindachneri* (Fig. 4.8), and *P. slevini* (Fig. 4.9) – previously known to occur in the Archipelago (Fig. 4). Since detailed descriptions of the latter six species are already available in the literature (Thomas, 1997; Van Denburgh, 1912), we provide extended descriptions below only for the three new species recognized here. We further provide as supplementary information a summary of quantitative external features and high-quality illustrations of type specimens (Figs S10–16, see supplemental material online) and hemipenes (Figs S17–19, see supplemental material online) for the remaining six Galápagos species.
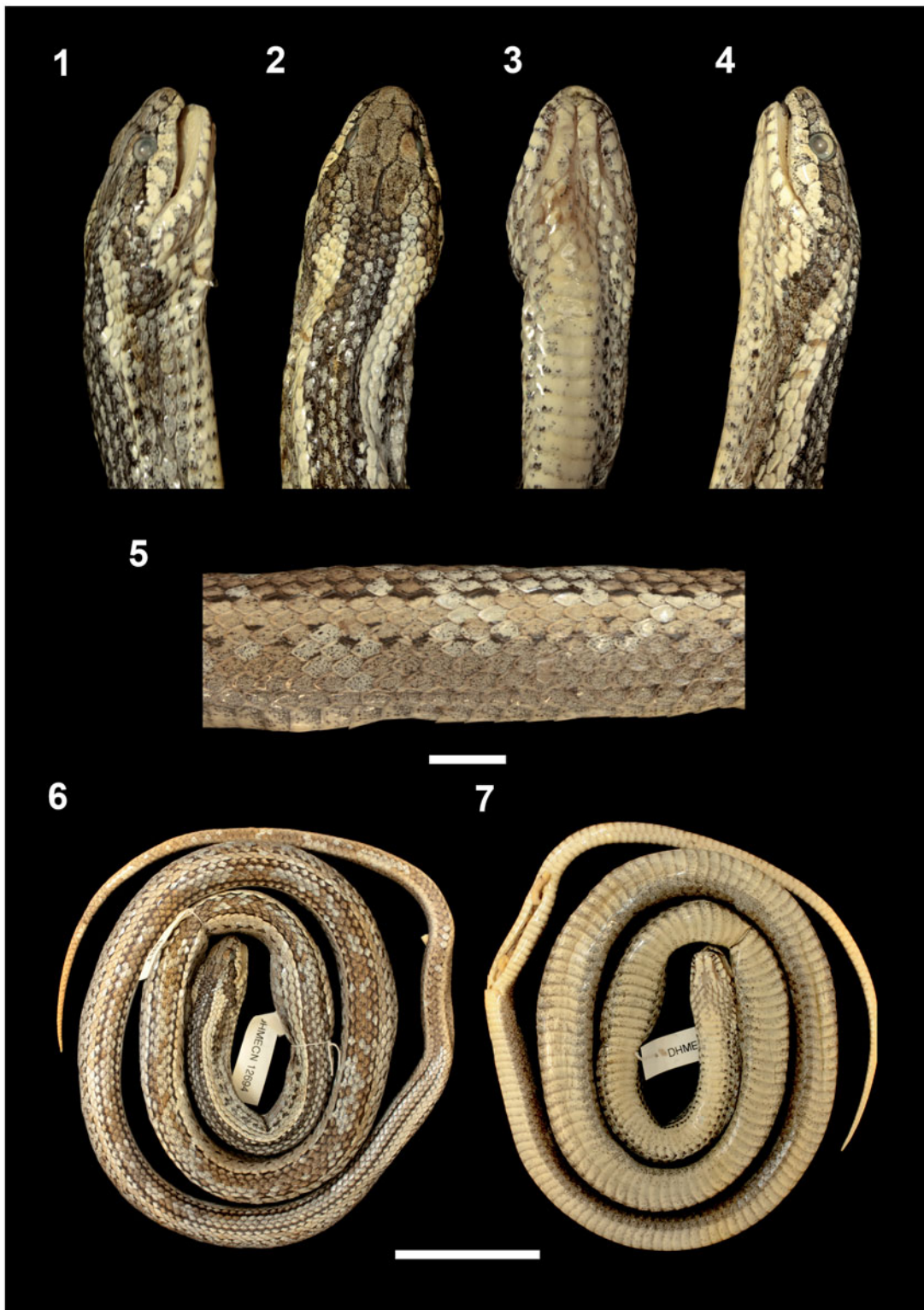
Pseudalsophis thomasi sp. nov.
Figs 4.5–4.6, 5, 6.1
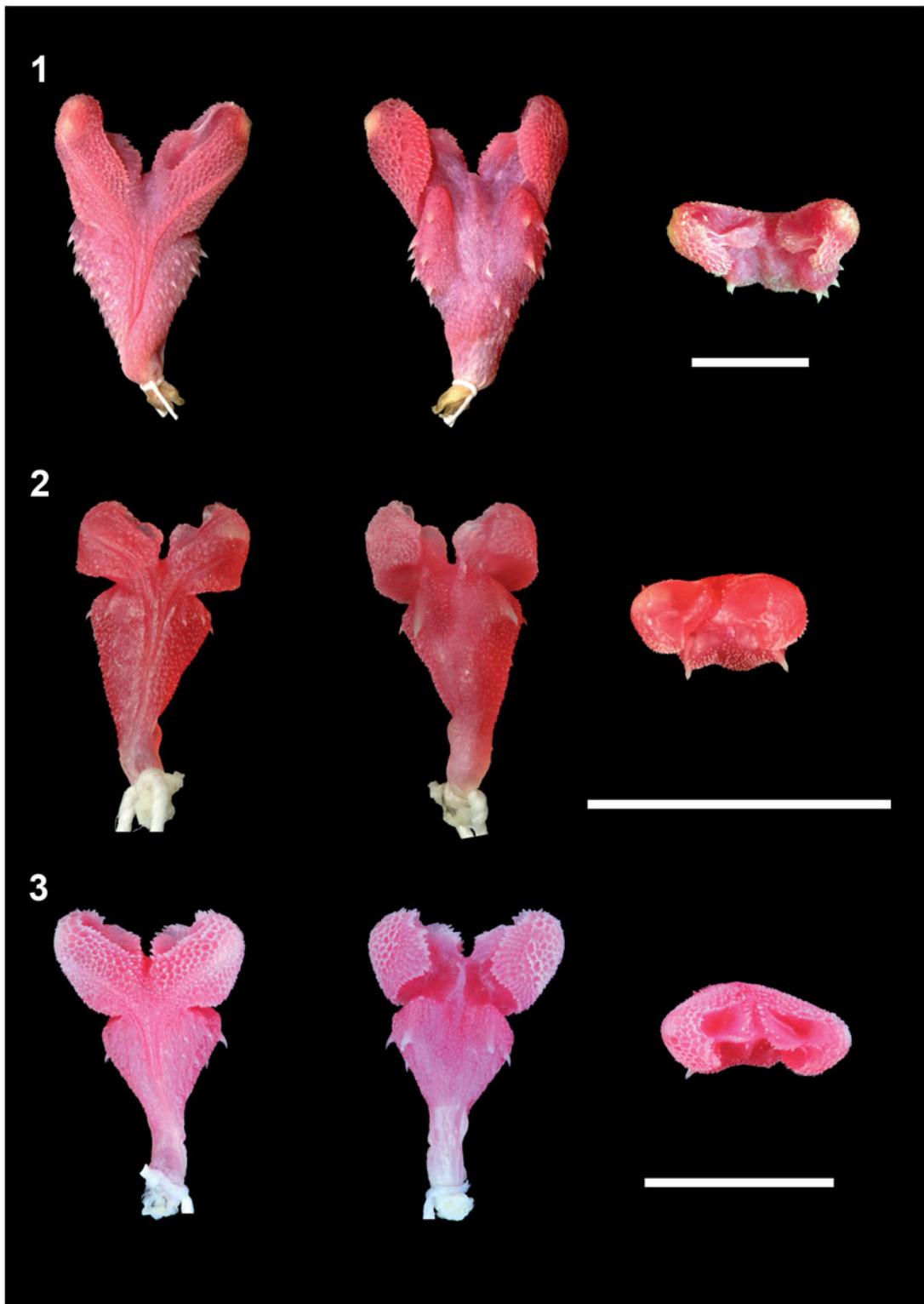
HOLOTYPE: DHMECN 12694 (Field number 1073), an adult male from Rábida Island (00°24′04″S, 90°42′28″W), collected on 18 June 2008 (Fig. 5).
PARATYPES: DHMECN 12696 (Field number 1071)♂, a male from Santiago Island, collected in the vicinities of Puerto Egas (00°14′33″N 90°51′34″W) on 17 June 2008; MZUSP 22557 (Field number 1065), a male from Santiago Island, collected in the vicinities of Puerto Egas (00°14′32″N 90°51′19″W) on 17 June 2008; MZUSP 22558 (Field number 1070), a female from Santiago Island, collected in the vicinities of Puerto Egas (00°14′38″N 90°51′25″W) on 17 June 2008; DHMECN 12695 (Field number 1074), a female from Rábida Island (00°23′58″N 90°42′23″W), collected on 18 June 2008; MZUSP 22556 (Field number 1072), a female from Rábida Island (00°24′04″N 90°42′28″W), collected on 18 June 2008.
ETYMOLOGY: A patronym honouring Robert A. Thomas for expanding our knowledge of the systematics and taxonomy of New World snakes.
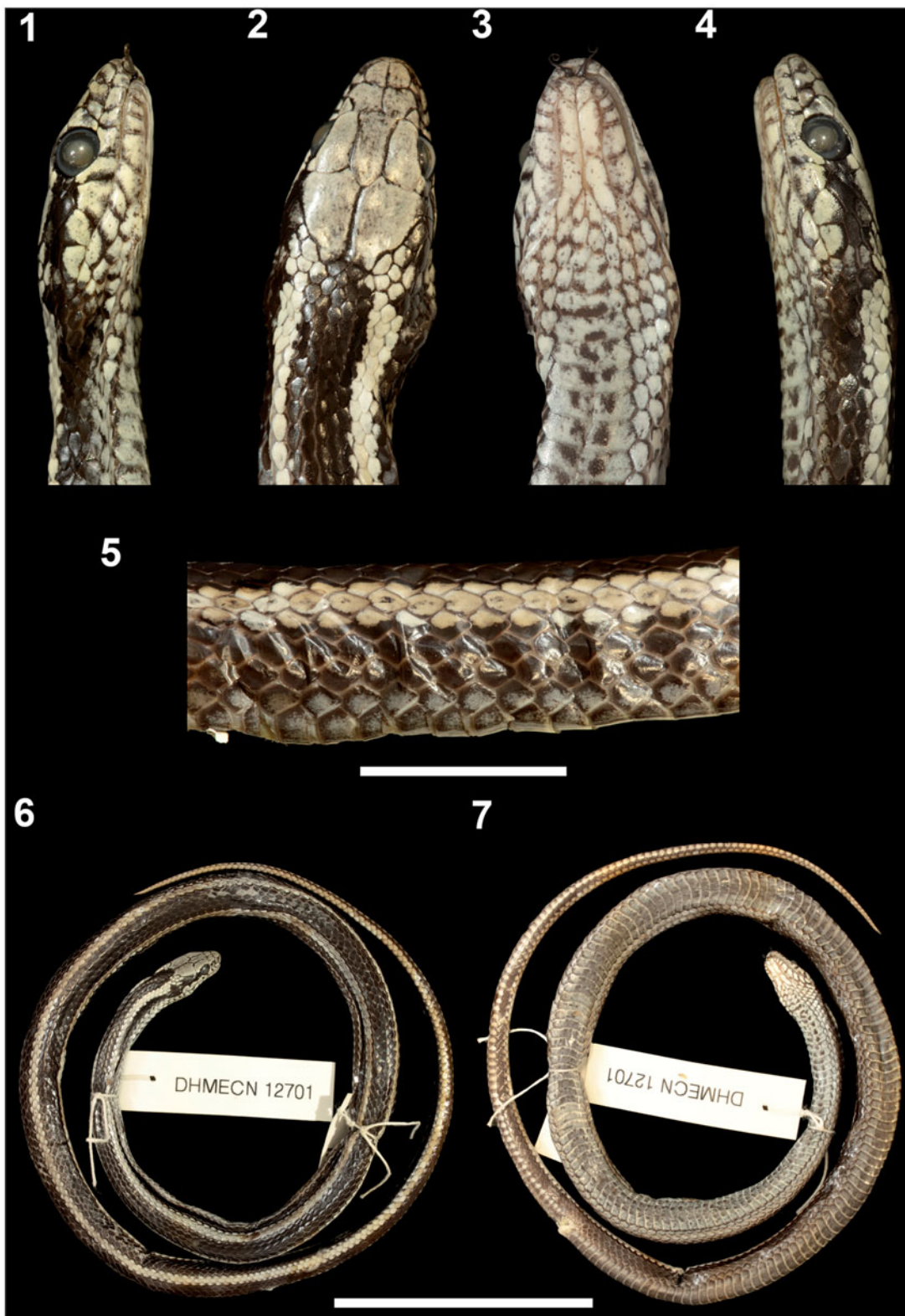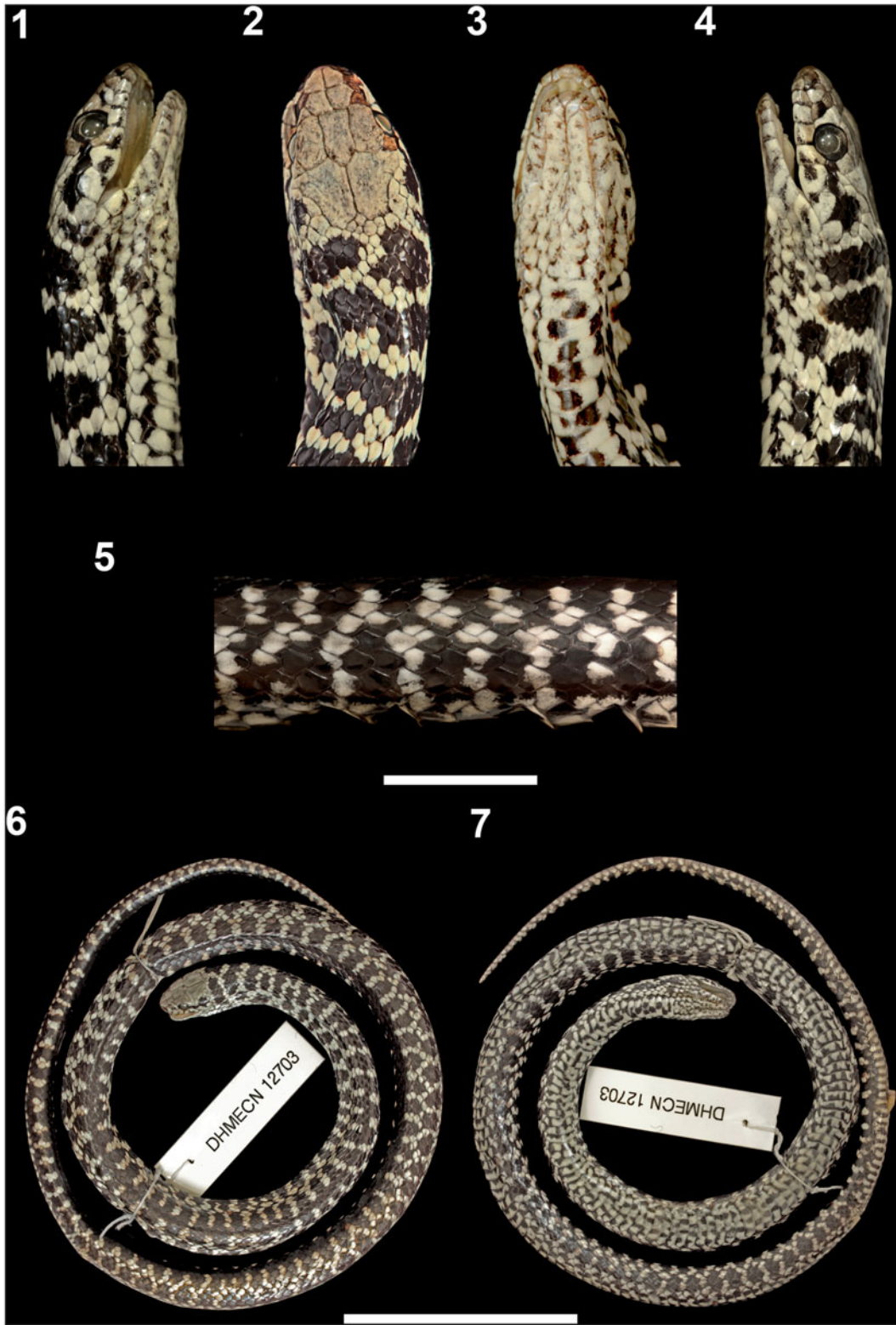
Figure 5. Holotype of *Pseudalsophis thomasi* sp. nov. (DHMECN 12696). Head in right lateral (7.1), dorsal (7.2), ventral (7.3), and left lateral (7.4) views; left lateral view of the body (7.7); specimen in dorsal (7.6) and ventral (7.7) views. Scales bars equal to 10 mm (above) and 50 mm (below), respectively.
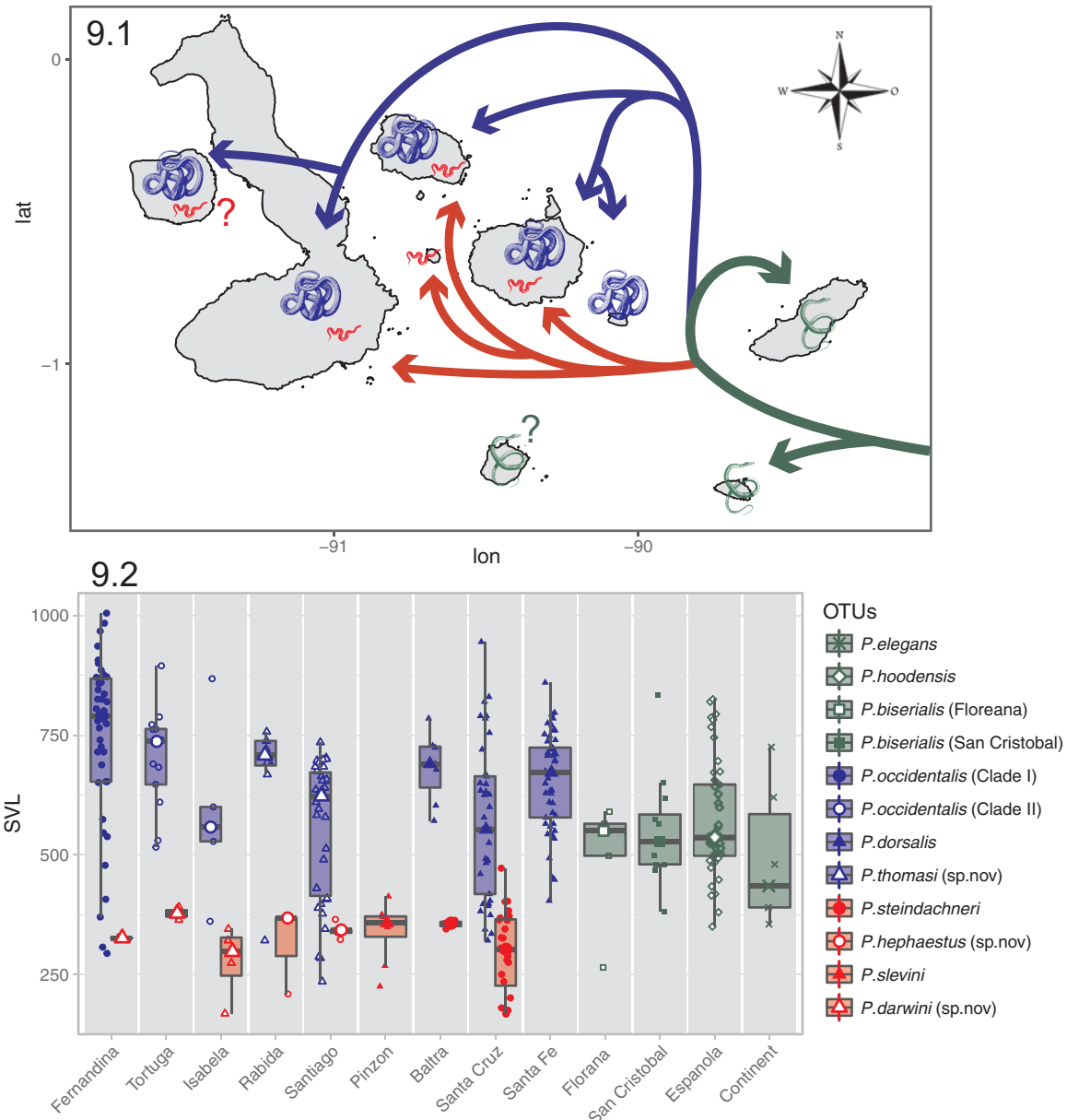
Figure 6. Hemipenes of *Pseudalsophis thomasi* sp. nov. (6.1), *Pseudalsophis hephaestus* sp. nov. (6.2), *Pseudalsophis darwini* sp. nov. (6.3). Left, sulcate view; middle, asulcate view; right, apical view.

Figure 7. Holotype of *Pseudalsophis hephaestus* sp. nov. (DHMECN 12701). Head in right lateral (7.1), dorsal (7.2), ventral (7.3), and left lateral (7.4) views; left lateral view of the body (7.7); specimen in dorsal (7.6) and ventral (7.7) views. Scales bars equal to 10 mm (above) and 50 mm (below), respectively.

Figure 8. Holotype of *Pseudalsophis darwini* sp. nov. (DHMECN 12701). Head in right lateral (7.1), dorsal (7.2), ventral (7.3), and left lateral (7.4) views; left lateral view of the body (7.7); specimen in dorsal (7.6) and ventral (7.7) views. Scales bars equal to 10 mm (above) and 50 mm (below), respectively.

Figure 9. Phylogenetic and morphological diversification of *Pseudalsophis* in the Galápagos Archipelago. The upper panel (9.1) depicts the phylogeny mapped onto the Archipelago's map. Silhouettes represent the continental (green); large insular (blue), and small insular (red) morphotypes recognized in this study, and their occurrences in the islands. Question marks indicate populations that are known to occur in a specific island but were not sampled for genetic material. The lower panel (9.2) shows the SVL for each population on each island, highlighting the occurrence of sympatry and morphological displacement. Colours correspond to the same morphotypes depicted in 9.1.

DIAGNOSIS: A large insular species of *Pseudalsophis* that differs from all other species of the genus by the following unique combination of characters: ventral counts in females 215–228 and males 212–224; subcaudal counts in males 97–108 and females 94–108; base of the lobular crest on the lobular crotch only slightly expanded when compared with *P. occidentalis* and *P. dorsalis*.

DESCRIPTION OF THE HOLOTYPE: The specimen is an adult male with 726 mm total length (TTL), 25.5 mm head length (2.7% of TTL) and 245 mm tail length (30% of TTL). Head gracile and distinct from neck, with 7.9 mm snout length (31% of HL); body robust, slightly wider than high. Dorsal scales in 19-19-17 rows, with two apical pits. There are 216 ventrals

(including 1 preventral), a divided anal, and 107 paired subcaudals. Rostral 1.95 times wider than high, and visible from above. Paired internasals 1.25 times longer than wide. Paired prefrontals as long as wide, in contact with each other and with internasal, nasal, loreal, preocular (right preocular damaged), supraocular, and frontal. Frontal pentagonal, 1.8 times longer than wide. Supraocular 2 times longer than wide. Parietals 1.6 times longer than wide. Nasal 1.9 times longer than high, in contact with supralabials 1–2 and divided above and below the naris. Loreal 1.85 times longer than high. Preocular 1.07 times higher than long (measured on the right preocular). Two small postoculars, the upper 1.6 times higher than the lower. One anterior and two posterior temporals, the anterior temporal in contact with both postoculars. Anterior temporal as long as wide. Lower posterior temporal 2 times longer than upper posterior temporal. Eight supralabials, 2–3 contact loreal, 4–5 border the orbit. Mental 1.9 times wider than long, separated from genials by first pair of infralabials. Ten infralabials, 1–5 in contact with anterior genials. Two anterior and two posterior genials 2.3 and 2.9 times longer than wide, respectively.

HEMIPENIS OF HOLOTYPE: The fully everted and maximally expanded hemipenis (Fig. 6.1) is deeply bilobed, bicalyculate, and semicapitate, with long lobes that are twice longer than wide in sulcate view. The forked sulcus spermaticus divides on the proximal half of the body. Each branch of the sulcus extends shortly in a centrolineal position along the distal half of the body, and diverges abruptly to take a centrifugal position on the lobes. Well-defined capitula cover the lobes on their sulcate, lateral, and asulcate sides. The capitula are formed by spinulate calyces that tend to decrease in size, gradually fading away proximally, towards the intrasulcar region of the lobes. The latter lacks calyces and intrasulcar spines, being ornamented only by sparsely distributed spinules. On the asulcate side of the lobes, the spinulate calyces of the capitulum are substituted by enlarged spinules with expanded fleshy bases that cover the proximal and medial one-third of the asulcate capitular surface. The edge of the capitulum is ornamented by a line of spinules. The asucate side of the capitulum has a rounded edge that overhangs the capitular groove. The internal (medial) surface of the lobes is mostly nude except for a conspicuous crest that extends from the base of the lobular crotch on the sulcate side to the distal edge of the capitulum medially, dividing the medial surface of the lobes in two distinct areas. The crest is inflated and conspicuous on its proximal two-third, constricting abruptly to form a thin fleshy ridge on its distal one-third. The expanded proximal half is covered with spinules while the small ridge is not ornamented. The nude area delimited by the crest and facing the sulcate side forms an extensive pocket visible in a sulcate view. The hemipenial body corresponds to two-thirds of the length of the organ, gradually constricting towards the base. The hemipenial body is covered with tiny spinules, except for a nude region in the distal part of the asulcate surface adjacent to the crotch. Eleven to 13 well-developed enlarged lateral spines are disposed on both sides of the distal half of the hemipenial body. The enlarged lateral spines fail to meet in the midline on the asulcate surface. A shallow proximal pocket is present, extending on the proximal half of the hemipenial body.

COLOURATION OF THE HOLOTYPE: The specimen has a brown head cap that extends as a vertebral band throughout the body, and a brown postocular stripe bordered ventrally by a black line that runs on the lower temporal region from the eye to the neck and throughout the lateral surface of the body. The black line disappears at the level of the last supralabial while the band tends to fade on the posterior half of the body. Labials and gular region are yellowish cream with infralabials bordered by black pigmentation. Dorsum with two large paravertebral light yellow longitudinal stripes that extend from the upper postocular to the anterior half of the tail, being 3 scales wide in the dorsum and 1–2 scales wide in the tail. The brown vertebral line is 5 scales wide in the dorsum and 2 scales wide in the tail, being bordered by black stripes throughout the body. The brown lateral pigmentation of the dorsum tends to fade gradually posteriorly, with the inner lines of scale rows assuming a lighter grey colour. The venter and underside of the tail are yellowish cream, and marked by sparsely distributed black spots that tend to concentrate on the lateral edges of ventral scales. In life, the specimen was yellow with a brown ground dorsum (Fig. 4.5).

VARIATION: largest specimen a male (DHMECN 12694) 983mm TTL, 245mm TL; largest female (CAS12153) 848mm TTL, 193mm TAL. Tail does not differ between males (23–26% of TTL; N = 11) and females (22–26%; N = 5). Ventral counts more numerous in females (215–228; x = 221.50; SD = 4.35; N = 10) than in males (212–224; x = 217.20; SD = 4.35; N = 20). Subcaudal counts divided throughout the tail and do not differ between males (97–108; x = 104.00; SD = 4.03; N = 9) and females (94–108; x = 99.6; SD = 5.59; N = 5).

NATURAL HISTORY: The holotype weighted 105 grams alive. The snake was active near the shore when caught around 10:00 in the morning. Paratype DHMECN 12696 regurgitated an adult female *Microlophus jacobi*. Live specimens of this species show two distinct colour morphs

in Santiago Island, one yellow (Fig. 4.5) and the other greyish-brown (Figs 4.5–6).

DISTRIBUTION: Santiago (James) and Rábida (Jervis) Islands, Galápagos Archipelago.

Pseudalsophis hephaestus sp. nov.
Figs 4.7, 6.2, 7

HOLOTYPE: DHMECN 12701 (Field number 1075), an adult male from Santiago Island, collected in front of the islet known as Sombrero Chino (00°21′55″S, 90°35′09″W) on 18 June 2008 (Fig. 7).

ETYMOLOGY: From the Greek Ηφαιστος (*Hephaestus*), name of the son of Zeus and Hera, God of fire and volcanoes (but also of blacksmiths, carpenters, and artisans), in allusion to the volcanic environment in which this species lives.

DIAGNOSIS: A small insular species of *Pseudalsophis* that differs from all other species of the genus by the following unique combination of characters: ventral counts in females 174–176 and males 177–183; subcaudal counts 87–114; edge of the capitulum on its asulcate side squared instead of rounded; capitular groove forming a sharp constriction on the organ. Further differs from *P. darwini* sp. nov. by its dorsum pattern of black vertebral and light paravertebral longitudinal bands.

DESCRIPTION OF THE HOLOTYPE: The specimen is an adult male with 468 mm total length (TTL), 13.3 mm head length (2.8% of TTL) and 142 mm tail length (30.3% of TTL). Head gracile and distinct from neck, with 3.7 mm snout length (27.8% HL); body robust, slightly wider than high. Dorsal scales in 19-19-17 rows, without apical pits. There are 178 ventrals (including 2 preventrals), a divided anal, and 100 paired subcaudals. Rostral 2.2 times wider than high, and visible from above. Paired internasals 1.4 times longer than wide. Paired prefrontals 1.05 times wider than long, in contact with each other and with internasal, nasal, loreal, preocular, supraocular, and frontal. Frontal pentagonal, 2.1 times longer than wide. Supraocular 1.9 times longer than wide. Parietals 1.5 times longer than wide. Nasal 1.8 times longer than high, in contact with supralabials 1–2 and divided above and below the naris. Loreal as long as high. Preocular 1.3 times higher than long. Two small postoculars, the upper 2.2 times higher than the lower. Two anterior and two posterior temporals. Upper anterior temporal in contact with both postoculars, and lower anterior temporal in contact with lower postocular. Lower anterior temporal 2.5 times longer than upper anterior temporal. Lower posterior temporal 1.1 times longer than upper posterior temporal. Eight supralabials, 2–3 contact loreal, 4–5 border the orbit. Mental 1.8 times wider than long, separated from genials by first pair of infralabials. Ten infralabials, 1–5

in contact with anterior genials. Two anterior and two posterior genials 3.4 and 3 times longer than wide, respectively.

HEMIPENIS OF HOLOTYPE: The fully everted and maximally expanded hemipenis (Fig. 6.2) is deeply bilobed, bicalyculate, and bicapitate, with short lobes that are as long as wide in sulcate view. The forked sulcus spermaticus divides on the distal half of the body. Each branch of the sulcus extends centrolineally throughout the organ and most of the surface of the lobes, reaching the laterodistal tip of the lobes in a centrifugal position. The lobes are covered by well-defined capitula that extend on the sulcate, lateral, and asulcate sides of the lobes. The capitula are formed by weakly developed and shallow spinulate calyces. The intrasulcar region of the lobes is mostly nude, lacking capitular calyces and intrasulcar spines. In the asulcate side of the lobes, the spinulate calyces of the capitulum are substituted by enlarged spinules with expanded fleshy bases that cover the proximal and medial half of the asulcate capitular surface. The edge of the capitulum is sparcely papillate. The edge of the capitulum on its asulcate side is squared instead of rounded and overhangs an extensive and deep capitular groove. The capitular groove creates a sharp constriction on the organ visible on a sulcate view. The internal (medial) surface of the lobes is nude except for a conspicuous, papillate crest (or ridge) that extends from the sulcate side of the lobular crotch to the distal edge of the capitulum, dividing the medial surface of the lobes in two distinct areas. The papillate crest forms an extensive nude pocket visible from a sulcate view. The hemipenial body corresponds to two-third of the length of the organ and is strongly constricted proximally and expanded distally, conferring a funil-shape condition to the organ. The hemipenial body is covered with tiny spinules, except for its proximal third that is nude. Four moderate-sized, enlarged lateral spines are present on both sides of the distal edge of the hemipenial body, just below the deep capitular grooves, being disposed circularly and forming a single row of spines. The last spine present on the asulcate side is significantly larger than the others. The enlarged lateral spines fail to meet in the midline on the asulcate side. A shallow proximal pocket is present on the proximal half of the hemipenial body.

COLOURATION OF THE HOLOTYPE: The specimen has a distinct light silver head cap that extends to the first dorsal scales posteriorly and edge of the parietals laterally, and a black postocular stripe that runs on the lower temporal region from the eye to the last supralabial scale, merging with the black dorsolateral band of the dorsum. Labials and gular region light silver, with sparse black markings concentrated on the posterior and

posterodorsal borders of the scales. Dorsum ground colour black, with two large paravertebral silver light longitudinal stripes that extend from the posterior edge of the parietals to the tip of the tail, being 2–3 scales wide in the dorsum and 2 scales wide in the tail. The black vertebral line formed between the edges of the two paravertebrals is 5 scales wide in the dorsum and 2–3 scales wide in the tail. The black pigmentation of the dorsum tends to fade gradually on its ventrolateral surface, with the first two lines of scale rows assuming a lighter grey colour, similar to the venter. The venter and underside of the tail are dark grey, with densely distributed irregular black dots and marks that cover most of the scale's surface. In the tail, subcaudals are light silver with black edges. In live specimens, the black body ground colour tends to be dark brown on the flanks and the two large paravertebral longitudinal stripes are light brown (Fig. 4.7).

VARIATION: Largest specimen a female (CAS10617) 536 mm TTL, 168 mm TAL; largest male (YPM6318) 515 mm TTL, 147 mm TAL. Tail does not differ between females (29–31% of TTL; N = 4) and males (29–31%; N = 2). Ventral counts more numerous in males (177–183; x = 179.60; SD = 2.19; N = 5) than in females (174–176; x = 175.33; SD = 1.15; N = 3). Subcaudal counts divided throughout the tail, and no difference evaluated between sexes (female: 96, N = 1; males: 87–114; x = 102.00; SD = 13.75; N = 3).

NATURAL HISTORY: The holotype weighed 12.8 grams alive. The snake was active near the shore when caught around 16:00 in the afternoon.

DISTRIBUTION: Santiago (James) and Rábida (Jervis) Islands, Galápagos Archipelago.

Pseudalsophis darwini sp. nov.
Figs 4.10, 6.3, 8

HOLOTYPE: DHMECN 12703 (field number 1049), an adult male from Tortuga Island (no GPS point registered), collected on 12 June 2008 (Fig. 8).

PARATYPES: DHMECN 12704 (Field number 1078), a male from Isabela Island, collected at Puerto Villamil on 21 June 2008; MZUSP 22564 (Field number 1064), a female from Isabela Island, collected at Piedra Blanca (00°07′27″N, 91°23′45″W) on 16 June 2008; MZUSP 22563 (Field number 1048), a female from Tortuga Island (no GPS point registered), collected on 12 June 2008.

ETYMOLOGY: The specific name, a noun in the genitive case, honours Charles Darwin for his invaluable contribution to our knowledge of the Galápagos Archipelago and to Science.

DIAGNOSIS: A small insular species of *Pseudalsophis* that differs from all other species of the genus by the following unique combination of characters: ventral counts in females 171–179 and males 175–181; subcaudal counts in females 82–94 and males 95–100; edge of the capitulum on its asulcate side squared instead of rounded; capitular groove forming a sharp constriction on the organ. Further differs from *P. hephaestus* sp. nov. by its dorsum colour pattern of transversal bands that are disposed in an inverted 'Y-shape' condition.

DESCRIPTION OF THE HOLOTYPE: The specimen is an adult male with 510 mm total length (TTL), 13.8 mm head length (2.7% of TTL) and 153 mm tail length (30% of TTL). Head gracile and distinct from neck, with 4.2 mm snout length (30.4% HL); body robust, slightly wider than high. Dorsal scales in 19-19-15 rows, without apical pits. There are 179 ventrals (including 1 preventral), a divided anal, and 95 paired subcaudals. Rostral 1.51 times wider than high, and visible from above. Paired internasals 1.4 times longer than wide. Paired prefrontals 1.1 times wider than long, in contact with each other and with internasal, nasal, loreal, preocular, supraocular, and frontal. Frontal pentagonal, 2.05 times longer than wide. Supraocular 1.6 times longer than wide. Parietals 1.3 times longer than wide. Nasal 1.6 times longer than high, in contact with supralabials 1–2 and divided above and below the naris. Loreal 1.2 times longer than high. Preocular 1.25 times higher than long. Two small postoculars, the upper 1.6 times higher than the lower. Two anterior and two posterior temporals. Upper and lower anterior temporal in contact with lower postocular. Lower anterior temporal 1.3 times longer than upper anterior temporal. Lower posterior temporal 1.4 times longer than upper posterior temporal. Eight supralabials, 2–3 contact loreal, 4–5 border the orbit. Mental 1.5 times wider than long, separated from genials by first pair of infralabials. Ten infralabials, 1–5 in contact with anterior genials. Two anterior and two posterior genials 2.5 and 2.7 times longer than wide, respectively.

HEMIPENIS OF THE HOLOTYPE: The fully everted and maximally expanded hemipenis (Fig. 6.3) is deeply bilobed, bicalyculate, and semicapitate, with short lobes that are as long as wide in sulcate view. The forked sulcus spermaticus divides on the distal half of the body. Each branch of the sulcus extends centrolineally throughout the organ and lobes, reaching the laterodistal tip of the lobes in a centrifugal position. The lobes are covered by well-defined capitula that extend on the sulcate, lateral, and asulcate sides of the lobes. The capitula are formed by spinulate calyces. The spinulate calyces tend to decrease in size, gradually fading away proximally, towards the intrasulcar region of the lobes. The

latter lacks intrasulcar spines. On the asulcate side of the lobes, the spinulate calyces of the capitulum are substituted by enlarged spinules with expanded fleshy bases, that cover all the proximal and medial half of the asulcate capitular surface, and expanded papillae, that form a fringe along the edge of the capitulum. The capitulum on its asulcate side has a peculiar square-shaped edge (instead of rounded) that overhangs an extensive and deep capitular groove. The capitular groove creates a sharp constriction on the organ that is visible on a sulcate view, and clearly defines both lobular and body regions. The internal (medial) surface of the lobes is mostly nude except for a conspicuous, thin papillate crest (or ridge) that extends from the sulcate side of the lobular crotch to the distal edge of the capitulum, dividing the medial surface of the lobes in two distinct areas. The nude area delimited by the papillate crest that faces the sulcate side tends to form an extensive pocket visible from a sulcate view. The hemipenial body corresponds to two-thirds of the length of the organ and is strongly constricted proximally and expands abruptly on its distal half, conferring a somewhat funil-shape condition to the organ. The hemipenial body is covered with tiny spinules, except for its proximal third that is nude. A few moderate-sized, enlarged lateral spines are present on both sides of the distal half of the hemipenial body, being restricted to four and eight spines on each side of the organ. The enlarged lateral spines fail to meet in the midline on the asulcate surface. A shallow proximal pocket is present, extending on the proximal half of the hemipenial body.

COLOURATION OF THE HOLOTYPE: The specimen has a distinct light brown head cap that extends to the first dorsal scales and a black postocular stripe that runs on the lower temporal region from the eye to the last supralabial scale, expanding on the temporal scales. Labials and gular region light brown and pale cream, respectively, with sparse black markings concentrated on the border of the scales. Dorsal ground colour light brown, with 83 dorsolateral black transversal bands that are 8–10 scales wide, and 77 black lateral blotches that are 2–3 scales wide. The dorsolateral transversal bands and lateral blotches are alternately disposed and separated by one scale-wide, light brown transversal bands that are disposed in an inverted 'Y-shape' condition on the flanks of the dorsum, conferring a variegated pattern to the body. The dorsolateral black transversal bands are fused on the vertebral row, forming a continuous longitudinal black vertebral band on the vertebral line that is 2–3 scales wide. Some dorsolateral transversal bands are asymmetrical, forming alternating dorsolateral bars on each side of the vertebral line. Both dorsolateral black transversal bands and lateral blotches fuse on the tail to form 48 black transversal bands. The venter and underside of the tail are light brown, with densely distributed irregular black dots and marks that cover most of the scale's surface. In the tail, the black marks are concentrated in the edge of the scales. In live specimens, the body ground colour tends to be lightly olive brown. However, the light olive tone is lost in preservative, leaving only a ground light brown colouration.

VARIATION: Largest specimen a female (MZUSP 22563) 543 mm TTL, 160 mm TAL; largest male (DHMECN 12703) 510 mm TTL, 153 mm TAL. Tail does not differ between males (29–30% of TTL; N = 3) and females (29–31%; N = 4). Ventral counts do not differ between males (175–181; x = 178.33; SD = 3.06; N = 3) and females (171–179; x = 175.75; SD = 3.40; N = 4). Subcaudal counts divided throughout the tail, higher in males (95–100; x = 97; SD = 2.65; N = 3) than in females (82–94; x = 88.25; SD = 5.06; N = 4).

NATURAL HISTORY: The holotype weighed 21 g alive. The snake was active when caught at the end of the day, around 16:00, on the steep outskirts of the island. The vegetation in the island is sparse and offers little protection for snakes.

DISTRIBUTION: Isabela (Albemarle), Fernandina (Narborough), and Tortuga (Brattle) Islands, Galápagos Archipelago. Only one specimen (CAS 4972) is known from Fernandina, but it conforms with *P. darwini*.

Divergence time estimation

The posterior probability trace of our BEAST analysis converged after 5 million generations, although values of ESS higher than 200 for all parameters were obtained after 30 million generations. Figure 3.1 shows our dated tree, with the newly described species added, indicating a late Miocene (6.9 Ma) age as the time of the Most Recent Common Ancestor (TMRCA) of all species of *Pseudalsophis*. The TMRCA of the whole Galápagos radiation was estimated within the early Pliocene (4.4 Ma). The age for coalescence of *P. biserialis* and subclades A and B was estimated around 3.6 Ma, closer to the middle Pliocene. Our analysis positioned the TMRCA between *P. biserialis* and subclade B also in the Pliocene (3.3 Ma). All other nodes for the cladogenetic process of *Pseudalsophis* in Galápagos were dated within the Quaternary. The TMRCA for subclade A (2.2 Ma) is more than twice older than the date estimated for subclade B (1.0 Ma). Particularly, the diversification of subclade A initiated within the Pleistocene, whereas subclade B diversified only in the late Pleistocene. Within subclade A, all the TMRCAs between species were older than the whole divergence of subclade B. The TMRCA for *P. hephaestus* and *P.*

slevini was estimated in the middle Pleistocene (1.3 Ma) while the TMRCA between these two species and *P. darwini* was dated within the early Pleistocene (1.8 Ma). Within subclade B, the date for coalescence between *P. dorsalis* and *P. thomasi* was estimated to be within the late Pleistocene (0.8 Ma).

Although our sampling was not designed for population inferences, our results indicate that besides the intraspecific divergence of *P. hoodensis*, dated in 0.7 Ma, all other species have a TMRCA of 0.3 Ma or less.

Discussion

Phylogenetic affinities within Dipsadidae

The Dipsadidae is the most species-rich snake family and a key element of the vertebrate Neotropical fauna. More recently, the two Asiatic genera *Thermophis* and *Stichophanes* were allocated in this mainly New World family (He, Feng, Liu, Guo, & Zhao, 2009; Wang, Messenger, Zhao, & Zhu, 2014). Our tree topology retrieves the two Asiatic genera *Thermophis* and *Stichophanes* as successive sister-groups of all the New World dipsadid radiation with strong bootstrap support (83%), supporting their inclusion in the family (Wang et al., 2014). This larger dipsadid clade is morphologically supported by two putative hemipenial synapomorphies previously thought to be present only in New World Dipsadids (body calyces on the asulcate surface of the lobes and lateral enlarged spines disposed on the sides of the hemipenial body) (Zaher, 1999). Our results further corroborate recent systematic studies of the family by retrieving with strong bootstrap support most of the previously hypothesized monophyletic tribes (Arteaga et al., 2017; Grazziotin et al., 2012; Hedges, Couloux, & Vidal, 2009; Pyron, Arteaga, Echevarría, & Torres-Carvajal, 2016; Pyron, Guayasamin, Peñafiel, Bustamante, & Arteaga, 2015; Vidal, Dewynter, & Gower, 2010; Zaher et al., 2009), with the exception of Alsophiini (*sensu* Hedges et al., 2009) and Saphenophiini (*sensu* Zaher et al., 2009). Hedges et al. (2009) recently diagnosed the tribe Alsophiini as a monophyletic dipsadid radiation with 10 genera, including *Uromacer*, and hypothesized a single dispersal event for the colonization of the Caribbean Islands. However, our results retrieve *Uromacer* outside the Caribbean clade, as the sister-group of the tribe Xenodontini, therefore corroborating Grazziotin et al.'s (2012: 457) alternative results and taxonomy (*contra* Hedges et al., 2009). Although it has poor bootstrap support, this topology reinforces the hypothesis of independent colonization of the Caribbean by at least two groups of Caribbean 'alsophiines' (Grazziotin et al., 2012).

The Saphenophiini, composed by the genera *Saphenophis* from Ecuador and Colombia, and *Pseudalsophis* from Ecuador, Chile, Peru, and Galápagos, was originally defined by Zaher et al. (2009) based on the presence of two putative hemipenial synapomorphies: the reduction or loss of ornamentation on the asulcate and medial surfaces of the hemipenial lobes, and the presence of a papillate ridge disposed proximo-distally in a lateral-to-medial orientation on the medial surface of each hemipenial lobe. However, despite hemipenial evidence, our ML tree does not support the tribe Saphenophiini as it stands (branches in red Fig. 1; Fig. S2, see supplemental material online). Since non-monophyly of Saphenophiini lacks statistical support in our analysis, we prefer to wait additional gene and taxon sampling to properly test its monophyly and suggest a more appropriate taxonomic change for the group.

Most of the more inclusive nodes of Dipsadidae were not strongly supported, and non-monophyly persists in a significant number of genera (*Synophis*, *Tretanorhinus*, *Hypsiglena*, *Sibon*, *Dipsas*, *Sibynomorphus*, *Geophis*, *Atractus*, *Thamnodynastes*, and *Oxyrhopus*) included in our analysis. Such results indicate that the diversity of Dipsadidae and the relationship among its components are far from resolved, despite significant advances made in the last decade. New methods capable of generating hundreds or thousands of loci, such as UCEs (Faircloth et al., 2012) or Anchored Phylogenomics (Lemmon, Emme, & Lemmon, 2012), should be applied to address short branches issues among well-corroborated Dipsadid tribes.

Among the few higher-level clades retrieved with moderate to strong support, an interesting and previously unnoticed pattern emerges suggesting that the Central and South American dipsadid radiations, as traditionally recognized, are paraphyletic in respect to each other (Fig. 1), with the Central American *Manolepis*, *Conophis*, and *Crisantophis* (Conophiini; Zaher et al., 2009) forming a clade that clusters with moderate support (78%) as the sister group of the South American dipsadids (Xenodontinae), while a South American clade formed by *Synophis* and *Diaphorolepis* (Diaphorolepidini; Pyron et al., 2015, 2016) clusters with strong support (83%) with the Central American dipsadids (Dipsadinae). These results emerge from recent advances in our knowledge of the phylogenetic affinities of these two poorly known lineages of New World snakes. Pyron et al. (2015, 2016) clarified the content of the tribe Diaphorolepidini, providing better grounds for the definition of their phylogenetic

affinities. Similarly, our ML tree recovered the tribe Conophiini as originally proposed by Zaher et al. (2009), including *Conophis* and *Manolepis* and with the genus *Crisantophis* nested in it as the sister group of *Conophis*. These results are perceived as an improvement over Grazziotin et al.'s (2012) analysis due to our better sampling of dipsadids and, although Conophiini (now including *Crisantophis*) received low support values, it is further corroborated by morphological similarities between *Crisantophis* and *Conophis* (Dunn, 1937; Villa, 1971) that highlights their close affinities and reinforces the hypothesis of monophyly of the group (*contra* Vidal et al., 2010). Higher-level affinities retrieved in our analysis between Diaphorolepini and Dipsadinae, on the one hand, and Conophiini and Xenodontinae, on the other hand, points to a more complex historical scenario of origin and diversification of the two main Central- and South-American dipsadid lineages than previously thought (Cadle, 1985; Cadle & Greene, 1993). Our results also recover a North American clade composed by the genera *Contia*, *Heterodon*, *Carphophis*, *Diadophis*, and *Farancia*. Despite low statistical support, this result corroborates earlier views (Cadle, 1984a,b,c, 1985; Zaher, 1999) of a monophyletic North American relictual snake lineage that clusters as the sister-group of remaining Neotropical dipsadids (Zaher et al., 2009; *contra* Pinou, Vicario, Marschner & Caccone, 2004).

As previously suggested by Zaher et al. (2009), our phylogenetic results corroborate the monophyly of *Pseudalsophis* as a maximally supported clade that includes the mainland *P. elegans* and all known Galápagos species (Fig. 1; Fig. S2, see supplemental material online). The genus is also supported by the presence of at least one putative hemipenial synapomorphy: the presence of a conspicuous papillate crest (or ridge) that extends from the sulcate side of the lobular crotch to the distal edge of the capitulum, dividing the medial surface of the lobes in two distinct areas and delimiting a nude pocket-like area that faces the sulcate side (Fig. 6; Figs S17–19; see supplemental material online). *Pseudalsophis* is not nested within Alsophiini or *Philodryas* (Thomas, 1997), but rather seems to be more closely related to the latter and to the tribe Xenodontini than to any other tribe of Dipsadidae. Our analysis recovers a weekly supported clade that includes the genera *Pseudalsophis*, *Psomophis*, and *Uromacer*, and the tribes Alsophiini and Xenodontini (Fig. 1; Fig. S2, see supplemental material online). This clade was first pointed out by Grazziotin et al. (2012) and appears recurrently in recent large-scale phylogenetic analyses (Figueroa, McKelvy, Grismer, Bell, & Lailvaux, 2016; Pyron, Burbrink, & Wiens, 2013), although without

Psomophis nested in it and with higher statistical support values (81% and 92% bootstrap support values, respectively). By confirming this hypothesis of relationship, our results also support the hypothesis that phylogenetic affinities of the genus *Pseudalsophis* lie with the continental South American dipsadid lineage (Zaher, 1999) instead of the Caribbean radiation (Thomas, 1997).

Both extended and reduced ML trees have *P. elegans* as the sister-group of a clade formed by all the insular species. However, the insular clade is strongly supported (82%) only in the extended ML tree. Among the insular species, *P. hoodensis* is the sister-group of a clade formed by *P. biserialis* and subclades A and B, formed by the small insular species *P. slevini* and *P. steindachneri* and the large insular species *P. dorsalis* and *P. occidentalis*, respectively. Although the latter clade is only weakly supported in both ML analyses, it is corroborated by at least one putative hemipenial synapomorphy: the presence of enlarged spinules with expanded fleshy bases covering the proximal and medial half of the asulcate capitular surface of the capitulum (Figs S17–19, see supplemental material online). This differentiated ornamentation on the asulcate side of the lobes is present but only weakly developed in P. hoodensis and P. elegans (Fig. S17, see supplemental material online).

Subclade A represents a very distinctive radiation of small-sized insular species that received maximal bootstrap support in our analysis. This clade is also corroborated by its uniquely derived hemipenial morphology, including a capitular groove that forms a sharp constriction of the organ at the base of the lobes, and a funil-shape hemipenial body that corresponds to two-thirds of the length of the organ (Fig. S18, see supplemental material online). Within subclade A, *Pseudalsophis steindachneri*, from the island of Santa Cruz, is the sister group of a strongly supported clade (82% bootstrap) that includes the remaining radiation of small insular species from the younger islands of Santiago, Rábida, Pinzón, Isabela, Fernandina, and Tortuga, and which includes *P. slevini* and two newly described species *P. hephaestus* and *P. darwini*. Although very similar externally (Figs 4.7–4.8), *P. steindachneri* and *P. hephaestus* differ significantly in their hemipenial morphology (Figs S18.2–18.4, see supplemental material online), especially in respect to the peculiar square-shaped condition of the capitulum of the latter species that is conspicuously distinct from the edge rounded shape present in *P. steindachneri*. Not surprisingly within Subclade A, the two species *P. heaphaestus* and *P. slevini* from islands of same age share a closer ancestor with each other than

with *P. darwini*, known to occur within the arch of younger islands.

Subclade A is retrieved as the sister group of a weakly supported clade formed by *P. biserialis* and Subclade B including *P. occidentalis*, *P. dorsalis* and the newly described *P. thomasi*. Similarly, *P. biserialis* is retrieved with weak support as the sister group of Subclade B. These results illustrate the unstable position of *P. biserialis*, a species that belongs to the arch of oldest islands in the present-day configuration of the Archipelago. Subclade B, on the other hand, is strongly supported (91%), and is also corroborated by the putative hemipenial synapomorphy of a spinulate lobular crest that is conspicuously expanded on the lobular crotch of the hemipenis (Fig. S19, see supplemental material online). Phylogenetic relationships between P. thomasi, P. dorsalis, and P. occidentalis are not fully resolved, with the latter two species forming only a weakly supported clade in our reduced ML analysis. Pseudalsophis thomasi and P. dorsalis differs significantly from each other in hemipenial morphology, and especially in respect to the conformation and degree of expansion of the lobular crest on the lobular crotch (Fig. S19, see supplemental material online).

Timing of arrival in the Galápagos

Here we provide an evolutionary hypothesis for the diversification of the Galápagos radiation of snakes inferred from our phylogenetic results and by taking into account the history of cladogenetic events, the estimated time of coalescence among lineages, and recent palaeogeographic models explaining the pattern of island emergence within the Galápagos Archipelago.

We estimated the age/time for the most recent common ancestor (TMRCA) of all extant species of *Pseudalsophis* at ∼6.9 Ma (± 3.7 myr). Although the current diversity of *Pseudalsophis* dates from the Late Miocene (∼6.9 Ma), the lineage is much older, originating in the Middle Miocene (∼14.8 Ma; ±4.8 myr) (Fig. S4; see supplemental material online). Our results suggest that *Pseudalsophis* colonized the Galápagos Archipelago through a single event of oceanic dispersal from the coast of South America between 6.9 Ma (TMRCA of *Pseudalsophis*) and 4.4 Ma (TMRCA of Galápagos snakes), near the Miocene/Pliocene boundary, by drifting via the Humboldt Current from the continent. The distribution of the mainland ancestor may have been similar to the extant species *P. elegans*, which occurs in the western Andes along the dry Pacific coast and inhabits coastal and interior desert areas (Myers & Hoogmoed, 1974).

The Humboldt Current is mainly driven by surface wind patterns (Sepulchre, Sloan, Snyder, & Fiechter, 2009). Such patterns were affected by several geological events during the Miocene and Pliocene (e.g., the uplift of the Andes, the closure of the Panama isthmus), rendering it difficult to determine the exact date the Humboldt Current assumed its present circulation pattern. However, it is probable that this event occurred during the late Miocene (Sepulchre et al., 2009). Accordingly, our results suggest that the Miocene/ Pliocene transition was a key period for Galápagos colonization by mainland snakes, although at this period of time none of the existing Galápagos Islands were emerged (Fig. 3.3).

Christie et al. (1992) argued that the time available for colonization of the Galápagos by terrestrial organisms is much longer than the age range of the existing islands, due to the existence of several drowned islands, often called 'Proto-Galápagos', that were emerged in the past, along the Carnegie ridge, as the product of a long-lived mantle hotspot. More recently, Geist, Snell, Snell, Goddard, and Kurz (2014) provided compelling evidence corroborating this hypothesis, based on direct age measurements of lavas present in the pre-existing islands, bathymetry of the Galápagos platform, and the estimated rate of movement of the Nazca plate. These authors found evidence to date the Proto-Galápagos islands to at least 9 Ma (Christie et al., 1992) and perhaps as long as 14 Ma (Werner et al., 1999). Geist et al. (2014) further hypothesized that the Pliocene/ Pleistocene Galápagos Archipelago had a much greater emerged area than the one visible today, adding to the existing 13 islands at least 19 other major islands that occurred as aerial landmasses between 1 and 5 Ma, but are currently submerged.

Therefore, colonization by *Pseudalsophis* must have occurred prior to the emergence of the presently existing islands, which are estimated to be no older than 4.0 to 3.5 Ma (Geist et al., 2014), supporting the hypothesis of colonization through drowned Proto-Galápagos landmasses (Geist, 1996). Dates of colonization older than the estimated age of the presently existing islands have been reported for other organisms (e.g., leaf-toed geckos, Torres-Carvajal, Barnes, Pozo-Andrade, Tapia, & Nicholls, 2014; weevils, Sequeira, Lanteri, Albelo, Bhattacharya, & Sijapati, 2008). These studies agree with the general palaeogeographic scenario described for Galápagos (Geist et al., 2014), and our study on *Pseudalsophis* also fits this scenario.

Taking the historical geological instability of the region into account, we propose a plausible scenario for the dispersal of the genus *Pseudalsophis* within the Galápagos Archipelago (Figs 2–3) that fits our resulting

calibrated phylogenetic frame. We based our interpretation on the 'progression rule' of Funk and Wagner (1995), which assumes that each island will be colonized by populations from the nearest older island, and that no extinctions and no 'back colonization' happen. Deviations from this model generate tree topologies that are not completely pectinate (unbalanced). Examples of the resulting tree topologies from deviant scenarios can be seen in Emerson (2002). Since the Galápagos Archipelago retains a pattern of older islands to the west and younger islands to the east, we also expect an east-to-west sequence of speciation events (Benavides, Baum, Snell, Snell, & Sites, 2009).

Our results indicate that the ancestor of all Galápagos snakes inhabited one of the Proto-Galápagos islands at ~4.4 Ma (± 2.2 myr). Individuals from this ancestral population dispersed from the Proto-Galápagos and colonized the islands of Española and San Cristóbal probably shortly after the emergence of these islands. However, based on our results, it is not clear which island was colonized first. It is also unclear which island is the oldest one (Geist et al., 2014), with Espanõla being dated as the oldest based on the age of subaerial lava (3 Ma), while San Cristóbal receives older dates based on the estimated movement of the Nazca Plate (4.0 Ma).

Despite the problems regarding the precise age estimation of these two islands (Geist et al., 2014; O'Connor, Stoffers, Wijbrans, & Worthington, 2007), our results indicate that the lineage that colonized the island of Española is currently represented only by *P. hoodensis*, whereas the lineage that colonized San Cristóbal is presently widespread throughout the archipelago. This scenario is well supported by our results since all the known species of *Pseudalsophis* from the Galápagos, except *P. hoodensis*, share an exclusive common ancestor at 3.6 Ma. Probably, this ancestor inhabited the island of San Cristóbal and colonized the other younger islands by dispersing from there as predicted by the 'progression rule'.

The first dispersion from San Cristóbal probably occurred towards the island of Santa Cruz between 3.6 and 2.2 Ma (Fig. 3.1). We suggest that the ancestral population of subclade A probably inhabited the island of Santa Cruz, since the only other emerged islands eastern to San Cristóbal during the Gelasian/Calabrian transition were Santa Fé (2.9 Ma) and Floreana (2.3–1.5 Ma), for which there is no evidence supporting the presence of the small insular morphotype. The estimated age of emergence for Santa Cruz is 2.3–1.1 Ma and the TMRCA of subclade A (Fig. 3.1) was estimated at ~2.2 Ma, indicating a rapid process of colonization after the island emergence. *Pseudalsophis* probably

dispersed from Santa Cruz towards Pinzón (1.7–1.3 Ma) between 1.8 and 1.3 Ma, and from there to Rábida (1.6–1.3 Ma) and Santiago (1.4–0.8 Ma). The TMRCA of *P. hephaestus*, *P. slevini*, and *P. darwini* was estimated at 1.8 Ma, which is older than the time of emergence of the corresponding islands of Santiago, Pinzón, and Isabela (0.8–0.5 Ma). Thus, the ancestor of these three species was probably present only in Santa Cruz. Here, we find evidence of a 'double colonization' pattern instead of the 'progression rule' (Emerson, 2002: Fig. 2b). Instead of being colonized by populations from Santiago, the island of Isabela was probably colonized by dispersion waves coming from the ancestral population present in Santa Cruz. A recent dispersion of *P. darwini* from Isabela colonized the islet of Tortuga during the end of the Pleistocene.

We conclude that the ancestral population that gave rise to the small (Subclade A) and large (Subclade B) radiations of insular species was probably restricted to San Cristóbal, since it represents the oldest island with species belonging to these two lineages (Fig. 3). Its presence in the Proto-Galápagos Island cannot be discarded too. Regardless which was the exact island inhabited by such ancestral population, to explain the colonization within subclade B we need to infer another deviation from the 'progression rule'. The TMRCA of *P. biserialis*, *P. occidentalis*, *P. dorsalis*, and *P. thomasi* was estimated at 3.3 Ma, and between 3.3 and 1 Ma, the colonization of the following similarly old islands took place: Santa Fé, Santa Cruz, Santiago, and Rábida (Isabela, Tortuga, and Fernandina were too young). It is impossible, based on our results, to determine which island was colonized first, but despite Santa Fé being the oldest island (2.9 Ma), we tend to favour the hypothesis of a primary colonization of Santa Cruz. Taking into account the topology of this clade (Figs 2–3.1), and the spatial distribution of the corresponding islands, we can explain the colonization process by assuming fewer steps if we infer a more central position for the ancestral population. This central position could allow the dispersion to different directions. Assuming Santa Cruz as the ancestral area, it was possible for the ancestral population to disperse to Isabela/Tortuga (between 1 and 0.4 Ma), and to Santiago and Rábida (between 0.8 and 0.1 Ma). Additionally, the presence of shared haplotypes (Fig. 3.2) between the *P. dorsalis* of Santa Fé and Santa Cruz (Seymour Norte) indicates a very recent dispersion between both islands, probably a 'back colonization' from a younger (Santa Cruz) to an older (Santa Fé) island.

Phenotypic evolution in the Galápagos snakes

Our clustering analysis highlights three broadly defined continental, large insular and small insular morphotypes.

Our phylogenetic analysis suggests that both large and small insular morphotypes correspond to well-supported monophyletic radiations (Fig. 1). On the other hand, the continental morphotype is a paraphyletic group, with *P. biserialis* nested within the clade otherwise composed of both large and small insular morphotypes (Subclades A and B). All hypothetical ancestors' phenotypes are classified as belonging to a specific morphotype with a posterior probability of ∼1.0. The phylogenetic analysis and ancestral state reconstruction show that the continental morphotype represent a plesiomorphic state for *Pseudalsophis*, being shared not only by *P. elegans*, the first diverging species (*P. hoodensis* and *P. biserialis*) and *P. occidentalis*, but by most hypothetical ancestral forms (Fig. 2). Both insular morphotypes, on the other hand, are shown to be apomorphic, each representing an independent transition from the continental morphotype that diversified posteriorly.

The three morphotypes show a very particular distribution on the Galápagos Islands. While the continental morphotype is distributed among the oldest islands (San Cristóbal, Floreana, Española), the small and large morphotypes co-occur on the younger islands (Santiago, Santa Cruz, Pinzon, Rabida, Isabela, and Fernandina). Each time that more than one species of *Pseudalsophis* is present on one island, it is always no more than two species, one being from the small morph and the other from the large morph (Fig. 9). Even though the continental morphotype is also large, there is no evidence of it coexisting along with species from the small morph. In almost all instances, small and large morphs are found in sympatry, with the exception of *P. slevini* at Pinzón.

Previous investigations on phenotypic evolution of insular snakes have shown that, while both increase and decrease in size are expected for insular species (Boback, 2003; Itescu et al., 2017), size increases tend to be to a smaller degree than size decreases. While our results are consistent with this pattern, it is not entirely clear why such size changes occurred. Snake size evolution is thought to be associated with island-specific factors, such as prey availability, competitors, predators, and island size and age (Itescu et al., 2017). However, the fact that two species with different sizes can co-exist on the same island shows that these island characteristics cannot fully explain the morphological differences between the two derived insular morphotypes.

The evolutionary history of the group and the pattern of distribution of species and phenotypes seen here could be potentially explained by two scenarios. The first is that both large and small derived morphs result from an evolutionary convergence to different adaptive regimes (Butler & King, 2004; Hansen, 1997) that are only present on younger islands. This hypothesis explains not only the differences between large and small morphs, but also the similarity among species which have hindered an accurate taxonomic identification of cryptic species without the use of molecular data (e.g., *P. steindachneri* and *P. hephaestus*). This is a probable explanation, given that smaller species seem to occur mainly on lava-deposits and use their smaller size to navigate through holes and cracks present in this environment (Fig. S20, see supplemental material online).

Alternatively, both large and small morphs may have evolved through character displacement triggered by intraspecific competition (Rice & Pfennig, 2010; Schluter, 2000). Since both insular morphs could have originated on Santa Cruz (see previous section), it is possible that intraspecific competition for resources could lead populations on that island to be subjected to different selective regimes on ecologically important traits, thus causing the sympatric speciation that led to both derived morphs. This could potentially be caused by restriction of resources in island habitats, a factor that could also exacerbate sexual dimorphism in order to alleviate intraspecific competition, a process that could be at play in *P. hoodensis* (Silva et al. 2017; Vincent, Herrel, & Irschick, 2004). Furthermore, derived morphs differ not only in terms of size, but also head size, a factor that might impact foraging performance (Andjelković, Tomović, & Ivanović, 2016; Segall, Cornette, Fabre, Godoy-Diana, & Herrel, 2016; Vincent, Dang, Herrel, & Kley, 2006). The existence of these morphs was then kept by niche conservatism through the remaining evolutionary history of the group, explaining not only why both insular morphotypes differ, but also why the large insular morphotype diverged from a similarly large plesiomorphic continental morphotype.

Testing these scenarios may be challenging for *Pseudalsophis*, given that both derived morphs form mutually monophyletic groups, constituting a 'worst case scenario' for investigation of causal factors in phylogenetic comparative tests (Felsenstein, 1985). In these cases, we lack phenotypic convergence and the signal of selection on phenotypic traits is profoundly conflated with evolutionary history, making the inference of the actual selective contribution to phenotypic evolution difficult to investigate. Nonetheless, further ecological, biomechanical, and quantitative genetics investigations could help to understand the causal factors underneath the distribution of taxa and phenotype of *Pseudalsophis* on the Galápagos Islands.

Acknowledgements

the specimens under their care: R. Drewes, J. Vindum, A. Leviton, R. Stoelting, J. Wilkinson, S. Blum (CAS), C. W. Myers, D. R. Frost, D. Kizirian (AMNH), K de Queiroz, R. McDiarmid, G. Zug (USNM), A. Dubois, A. Ohler, I. Ineich, R. Bour (MNHN), D. Gower, M. Wilkinson, P. Campbell (BMNH), H. Grillitsch (NMW). We are deeply indebted to D. Gower, H. Grillitsch, and M. G. Pires for kindly sending photographs of the type specimens of *P. dorsalis* and *P. biserialis*. We are grateful to M. Gardener, G. Jiménez (Charles Darwin Foundation), V. Carrión G., R. Molina Moreira, R. Valle, W. Tapia, V. Cedeño Escobar, R. Boada, and S. Villamar (Parque Nacional Galápagos) who provided support for field and laboratory research in the Galápagos, including permit authorizations. We are especially grateful to L. Lobo, S. Villamar and C. Marques who participated in the fieldwork, and to R. A. Thomas who helped with meristic counts of specimens housed at the California Academy of Sciences and kindly offered his notes on Galápagos species. We would like to extend our gratitude to the staff of the Colégio Humboldt, San Cristóbal Island, who allowed us to examine the scientific collection from their institution, and the crew of the boat *Queen Mabel* who conducted our expedition through the islands of the Archipelago.

Supplemental data

Supplemental data for this article can be accessed here: http://dx.doi.org/10.1080/14772000.2018.1478910

ORCID

HUSSAM ZAHER http://orcid.org/0000-0002-6994-489X
MARIO H. YÁNEZ-MUÑOZ http://orcid.org/0000-0003-3224-1987
MIGUEL T. RODRIGUES http://orcid.org/0000-0003-3958-9919
ROBERTA GRABOSKI http://orcid.org/0000-0002-9123-4819
FABIO A. MACHADO http://orcid.org/0000-0002-0215-9926
MARCO ALTAMIRANO-BENAVIDES http://orcid.org/0000-0002-3082-8103
SANDRO L. BONATTO http://orcid.org/0000-0002-0064-467X
FELIPE G. GRAZZIOTIN http://orcid.org/0000-0001-9896-9722

References

Aktas, C. (2015). Haplotypes: Haplotype inference and statistical analysis of genetic variation (version 1.0) *[R package]*. Retrieved from https://CRAN.R-project.org/package=haplotypes (accessed 16 May 2018).

Andjelković, M., Tomović, L., & Ivanović, A. (2016). Variation in skull size and shape of two snake species (*Natrix natrix* and *Natrix tessellata*). *Zoomorphology*, *135*, 1–11.

Arnold, S. J., & Phillips, P. (1999). Hierarchical comparison of genetic variance-covariance matrices. II. Coastal-inland divergence in the garter snake, *Thamnophis elegans*. *Evolution*, *53*, 1516–1527.

Arteaga, A., Mebert, K., Valencia, J. H., Cisneros-Heredia, D. F., Peñafiel, N., Reyes-Puig, C., … Guayasamin, J. M. (2017). Molecular phylogeny of *Atractus* (Serpentes, Dipsadidae), with emphasis on Ecuadorian species and the description of three new taxa. *ZooKeys*, *661*, 91–123.

Beebe, W. (1924). *Galápagos: Word's End*. New York: Putnam & Sons.

Benavides, E., Baum, R., Snell, H. M., Snell, H. L., & Sites Jr., J. W. (2009). Island biogeography of Galápagos lava lizards (Tropiduridae: *Microlophus*): Species diversity and colonization of the archipelago. *Evolution*, *63*, 1606–1626.

Boback, S. M. (2003). Body size evolution in snakes: Evidence from island populations. *Copeia*, *1*, 81–94.

Bouckaert, R. & Drummond, A. J. (2017). bModelTest: Bayesian phylogenetic site model averaging and model comparison. *BioMedCentral Evolutionary Biology*, *17*, 42.

Bouckaert, R., Heled, J., Kühnert, D., Vaughan, T., Wu, C-H., Xie, D., … Drummond, A. J. (2014). BEAST 2: A software platform for Bayesian evolutionary analysis. *Public Library of Science Computational Biology*, *10*, e1003537. https://doi.org/10.1371/journal.pcbi.1003537

Butler, M. A., & King, A. (2004). Phylogenetic comparative analysis: A modeling approach for adaptive evolution. *American Naturalist*, *164*, 683–695.

Butts, C. T. (2015). network: Classes for Relational Data. The StatnetProject (http://statnet.org) (version 1.13.0) *[R package]*. Retrieved from http://CRAN.R-project.org/package=network (accessed 16 May 2018).

Butts, C. T. (2016). *sna: Tools for Social Network Analysis.* (version 2.4) *[R package]*. Retrieved from https://CRAN.R-project.org/package=sna (accessed 16 May 2018).

Cadle, J. E. (1984a). Molecular systematics of Neotropical xenodontine snakes: I. South American xenodontines. *Herpetologica*, *40*, 8–20.

Cadle, J. E. (1984b). Molecular systematics of Neotropical xenodontine snakes: II. Central American xenodontines. *Systematics Zoology*, *34*, 1–20.

Cadle, J. E. (1984c). Molecular systematics of Neotropical xenodontine snakes. III. Overview of xenodontine phylogeny and the history of New World snakes. *Copeia*, *1984*, 641–652.

Cadle, J. E. (1985). The Neotropical colubrid snake fauna (Serpentes: Colubridae): Lineage components and biogeography. *Herpetologica*, *40*, 8–20.

Cadle, J. E., & Greene H. W. 1993. Phylogenetic patterns, biogeography, and the ecological structure of Neotropical snake assemblages. In R. E. Ricklefs & D. Schluter (Eds.), *Species diversity in ecological communities* (pp. 281–293). Chicago: The University of Chicago Press.

Carvalho, A. L. G., Sena, M. A., Peloso, P. L. V., Machado, F. A., Montesinos, R., Silva, H. R., … Rodriges, M. T. (2016). A New *Tropidurus* (Tropiduridae) from the Semiarid Brazilian Caatinga: Evidence for conflicting signal between mitochondrial and nuclear loci affecting the phylogenetic reconstruction of South American collared lizards. *American Museum Novitates*, *3852*, 1–68.

Christie, D. M., Duncan, R. A., McBirney, A. R., Richards, M. A., White, W. M., Harp, K. S., & Fox, C. G. (1992). Drowned islands downstream from the Galápagos hotspot imply extended speciation times. *Nature*, *355*, 246–248.

Dowling, H. (1951). A proposed method of expressing scale reductions in snakes. *Copeia*, *1951*, 131–134.

Dunn, E. R. (1937). New or unnamed snakes from Costa Rica. *Copeia*, *1937*, 213–215.

Emerson, B. C. (2002). Evolution on oceanic islands: Molecular phylogenetic approaches to understanding pattern and process. *Molecular Ecology*, *11*, 951–966.

Faircloth, B. C., McCormack, J. E., Crawford, N. G., Harvey, M. G., Brumfield R. T., & Glenn T. C. (2012). Ultraconserved elements anchor thousands of genetic markers spanning multiple evolutionary timescales. *Systematic Biology*, *61*, 717–726.

Felsenstein, J. (1985). Phylogenies and the comparative method. *American Naturalist*, *125*, 1–15.

Figueroa, A., McKelvy, A. D., Grismer, L. L., Bell, C. D., & Lailvaux, S. P. (2016). A species-level phylogeny of extant snakes with description of a new colubrid subfamily and genus. *Public Library of Science One*, *11*, e0161070.

Funk, V. A., & Wagner, W. L. (1995). Biogeographic patterns in the Hawaiian Islands. In W. L. Wagner & V. A. Funk (Eds.), *Hawaiian biogeography: Evolution on a hot spot Archipelago* (pp. 379–419). Washington: Smithsonian Institution Press.

Geist, D. (1996). On the emergence and submergence of the Galápagos Islands. *Noticias de Galápagos*, *56*, 5–8.

Geist, D., Snell, H., Snell, H., Goddard, C., & Kurz, M. (2014). Paleogeography of the Galápagos Islands and biogeographical implications. In K. Harpp, E. Mittelstaedt, N. d'Ozouville & D.W. Graham (Eds.), *The Galápagos: a natural laboratory for the earth sciences* (pp. 145–166). Washington: American Geophysical Union.

Grazziotin, F. G., Zaher, H., Murphy R. W., Scrocchi, G., Benavides, M. A., Zhang, Y. P., & Bonatto, S. L. (2012). Molecular phylogeny of the new world Dipsadidae (Serpentes: Colubroidea): a reappraisal. *Cladistics*, *28*, 437–59.

Hansen, T. (1997). Stabilizing selection and the comparative analysis of adaptation. *Evolution*, *51*, 1341–1351.

He, M., Feng, J.-C., Liu, S.-Y., Guo, P., & Zhao, E.-M. (2009). The phylogenetic position of *Thermophis* (Serpentes: Colubridae), an endemic snake from the Qinghai-Xizang plateau, China. *Journal of Natural History*, *43*, 479–488.

Hedges, S. B., Couloux, A., & Vidal, N. (2009). Molecular phylogeny, classification, and biogeography of West Indian racer snakes of the tribe Alsophiini (Squamata, Dipsadidae, Xenodontinae). *Zootaxa*, *2067*, 1–28.

Itescu, Y., Schwarz, R., Donihue, C. M., Slavenko, A., Roussos, S. A., Sagonas, K., … & Meiri, S. (2018). Inconsistent patterns of body size evolution in co-occurring island reptiles. *Global Ecology and Biogeography*, *69*, 473–513. http://doi.org/10.1111/geb.12716

Katoh, K., Kuma, K., Toh, H., & Miyata, T. (2005). MAFFT version 5: Improvement in accuracy of multiple sequence alignment. *Nucleic Acids Research*, *33*, 511–518.

Kearse, M., Moir, R., Wilson, A., Stones-Havas, S., Cheung, M., Sturrock, S., … Drummond, A. (2012). Geneious Basic: An integrated and extendable desktop software platform for the organization and analysis of sequence data. *Bioinformatics*, *28*, 1647–1649.

Lanfear, R., Frandsen, P. B., Wright, A. M., Senfeld, T., & Calcott, B. (2016). PartitionFinder 2: New methods for selecting partitioned models of evolution for molecular and morphological phylogenetic analyses. *Molecular Biology and Evolution*, *34*, 772–773.

Lemmon, A. R., Emme, S. A., & Lemmon, E. M. (2012). Anchored hybrid enrichment for massively high-throughput phylogenomics. *Systematic Biology*, *61*, 727–744.

Lindell, L. E. (1994). The evolution of vertebral number and body size in snakes. *Functional Ecology*, *8*, 708–719.

Machado, F. A., & Hingst-Zaher, E. (2009) Investigating South American biogeographic history using patterns of skull shape variation on *Cerdocyon thous* (Mammalia: Canidae). *Biological Journal of the Linnean Society*, *98*, 77–84.

Merlen, G., & Thomas R. A. (2013). A Galápagos ectothermic terrestrial snake gambles a potential chilly bath for a protein-rich dish of fish. *Herpetological Review*, *44*, 415–417.

Molina, F. B., Machado, F. A., & Zaher, H. (2012). Taxonomic validity of *Mesoclemmys heliostemma* (McCord, Joseph-Ouni & Lamar, 2001) (Testudines, Chelidae) inferred from morphological analysis. *Zootaxa*, *3575*, 63–77.

Myers, C. W. (2003). Rare snakes – five new species from eastern Panamá: Reviews of northern *Atractus* and southern *Geophis* (Colubridae: Dipsadinae). *American Museum Novitates*, *3391*, 1–47.

Myers, C. W., & Cadle, J. E. (2003). On the snake hemipenis, with notes on *Psomophis* and techniques of eversion: A response to Dowling. *Herpetological Reviews*, *34*, 295–302.

Myers, C. W., & Hoogmoed, M. S. (1974). Zoogeographic and taxonomic status of the South American snake *Tachymenis surinamensis* (Colubridae). *Zoologische Mededelingen*, *48*, 187–195.

Noonan, B. P., & Chippindale, P. T. (2006). Dispersal and vicariance: The complex evolutionary history of boid snakes. *Molecular Phylogenetics and Evolution*, *40*, 347–358.

O'Connor, J. M., Stoffers, P., Wijbrans, J. R., & Worthington, T. J. (2007), Migration of widespread long-lived volcanism across the Galápagos Volcanic Province: Evidence for a broad melting anomaly? *Earth and Planetary Science Letters*, *263*, 339–354.

Phillips, P., & Arnold, S. J. (1999). Hierarchical comparison of genetic variance-covariance matrices. I. Using the Flury hierarchy. *Evolution*, 53, 1506–1515.

Pinou, T., Vicario, S., Marschner, M., & Caccone, A. (2004). Relict snakes of North America and their relationships within Caenophidia, using likelihood-based Bayesian methods on mitochondrial sequences. *Molecular Phylogenetics and Evolution*, 32, 563–574.

Pyron R. A., Arteaga A., Echevarría L. Y., & Torres-Carvajal, O. (2016). A revision and key for the tribe Diaphorolepidini (Serpentes: Dipsadidae) and checklist for the genus *Synophis*. *Zootaxa*, 4171, 293–320.

Pyron R. A., Burbrink F. T., & Wiens J. J. (2013). A phylogeny and revised classification of Squamata, including 4161 species of lizards and snakes. *BioMed Central Evolutionary Biology*, 13, 93.

Pyron, R. A., Guayasamin, J. M., Peñafiel, N., Bustamante, L., & Arteaga, A. (2015). Systematics of Nothopsini (Serpentes, Dipsadidae), with a new species of *Synophis* from the Pacific Andean slopes of southwestern Ecuador. *ZooKeys*, 541, 109–147.

Rambaut A., Suchard M. A., Xie, D., & Drummond A. J. (2014). *Tracer* (version 1.6). Retrieved from http://tree.bio.ed.ac.uk/software/tracer/ (accessed 16 May 2018).

Rice, A. M., & Pfennig, D. W. (2010). Does character displacement initiate speciation? Evidence of reduced gene flow between populations experiencing divergent selection. *Journal of Evolutionary Biology*, 23, 854–865. http://doi.org/10.1111/j.1420-9101.2010.01955.x

Schluter, D. (2000). Ecological character displacement in adaptive radiation. *The American Naturalist*, 156, 4–16.

Schluter, D., Price, T., Mooers, A.Ø., & Ludwig, D. (1997). Likelihood of ancestor states in adaptive radiation. *Evolution*, 51, 1699–1711.

Segall, M., Cornette, R., Fabre, A.-C., Godoy-Diana, R., & Herrel, A. (2016). Does aquatic foraging impact head shape evolution in snakes? *Proceedings of the Royal Society of London B*, 283, 20161645–20161648. http://doi.org/10.1098/rspb.2016.1645

Sepulchre, P., Sloan, L. C., Snyder, M., & Fiechter, J. (2009). Impacts of Andean uplift on the Humboldt Current system: A climate model sensitivity study. *Paleoceanography and Paleoclimatology*, 24, PA4215.

Sequeira, A. S., Lanteri, A. A., Albelo, L. R., Bhattacharya, S., & Sijapati, M. (2008) Colonization history, ecological shifts and diversification in the evolution of endemic Galápagos weevils. *Molecular Ecology*, 17, 1089–1107.

Silva, F. M., de Oliveira, L. S., Nascimento, L. R., Machado, F. A. & Prudente, A. L. (2017). Sexual dimorphism and ontogenetic changes of Amazonian pit vipers (*Bothrops atrox*). *Zoologischer Anzeiger*, 271, 15–24. http://doi.org/10.1016/j.jcz.2017.11.001

Slevin, J. R. (1935). An account of the reptiles inhabiting the Galápagos Islands. *Bulletin New York Zoological Society*, 38, 3–25.

Stamatakis, A. (2014). RAxML version 8: A tool for phylogenetic analysis and post-analysis of large phylogenies. *Bioinformatics*. 30, 1312–1313.

Thomas, R. A. (1997). Galápagos terrestrial snakes: Biogeography and systematics. *Herpetological Natural History*. 5, 19–40.

Torres-Carvajal, O., Barnes, C. W., Pozo-Andrade, M. J., Tapia, W., & Nicholls, G. (2014). Older than the islands: Origin and diversification of Galápagos leaf-toed geckos (Phyllodactylidae: *Phyllodactylus*) by multiple colonizations. *Journal of Biogeography*, 41, 1883–1894.

Van Denburgh, J. (1912), Expedition of the California Academy of Sciences to the Galápagos Islands, 1905-1906: IV. The Snake of the Galápagos Islands. *Proceedings of the California Academy of Sciences*, 1, 323–374.

Vidal, N., Dewynter, M., & Gower, D. J. (2010). Dissecting the major American snake radiation: A molecular phylogeny of the Dipsadidae Bonaparte (Serpentes, Caenophidia). *Comptes Rendus Biologies*, 333, 48–55.

Villa, J. (1971). *Crisantophis*, a new genus for *Conophis nevermanni* Dunn. *Journal of Herpetology*, 5, 173–177.

Vincent, S. E., Dang, P. D., Herrel, A., & Kley, N. J. (2006). Morphological integration and adaptation in the snake feeding system: A comparative phylogenetic study. *Journal of Evolutionary Biology*, 19, 1545–1554. http://doi.org/10.1111/j.1420-9101.2006.01126.x (accessed 16 May 2018).

Vincent, S. E., Herrel, A., & Irschick D. J. 2004. Sexual dimorphism in head shape and diet in the cottonmouth snake (*Agkistrodon piscivorus*). *Journal of Zoology, London*, 264, 53–59.

Wang, X. Messenger, K., Zhao, E., Zhu, C. (2014). Reclassification of *Oligodon ningshaanensis* Yuan, 1983 (Ophidia: Colubridae) into a new genus, *Stichophanes* gen. nov. with description on its malacophagous behavior. *Asian Herpetological Research*, 5, 137–149.

Werner, R., Hoernle, K., Van Den Bogaard, P., Ranero, C., von Huene R., & Korich, D. (1999). Drowned 14-my.-old Galápagos archipelago off the coast of Costa Rica: Implications for tectonic and evolutionary models. *Geology*, 27, 499–502.

Zaher, H. (1999). Hemipenial morphology of the South American xenodontine snakes: With a proposal for a monophyletic Xenodontinae and a reappraisal of colubroid hemipenes. *Bulletin of the American Museum of Natural History*, 240, 1–168.

Zaher, H., & Prudente, A. L. (2003). Hemipenes of *Siphlophis* (Serpentes, Xenodontinae) and techniques of hemipenial preparation in snakes: A response to Dowling. *Herpetological Review*, 34, 302–306.

Zaher, H., Grazziotin, F. G., Cadle, J. E., Murphy, R. W., Moura-Leite, J. C., & Bonatto, S. L. (2009). Molecular phylogeny of advanced snakes (Serpentes, Caenophidia) with an emphasis on South American Xenodontines: A revised classification and descriptions of new taxa. *Papéis Avulsos de Zoologia (São Paulo)*, 49, 115–153.

Zuur, A. F., Ieno, E. N., & Elphick, C. S. (2010). A protocol for data exploration to avoid common statistical problems. *Methods in Ecology and Evolution*, 1, 3–14. http://doi.org/10.1111/j.2041-210X.2009.00001.x

Associate Editor: Mark Wilkinson